

Nano-Petrophysical Studies of Avalon-Bone Spring-Wolfcamp and Dean-Sprayberry-Wolfcamp Shale Systems*

(Max) QinHong Hu¹, Collin Adon¹, Sam Becker¹, Jordan Bevers¹, Ashley Chang¹, Ryan Jones¹, Griffin Mann¹, Benton Mowrey¹, Nabil Mzee¹, Ryan Quintero¹, and Ben Rogers¹

Search and Discovery Article #51688 (2021)**

Posted February 8, 2021

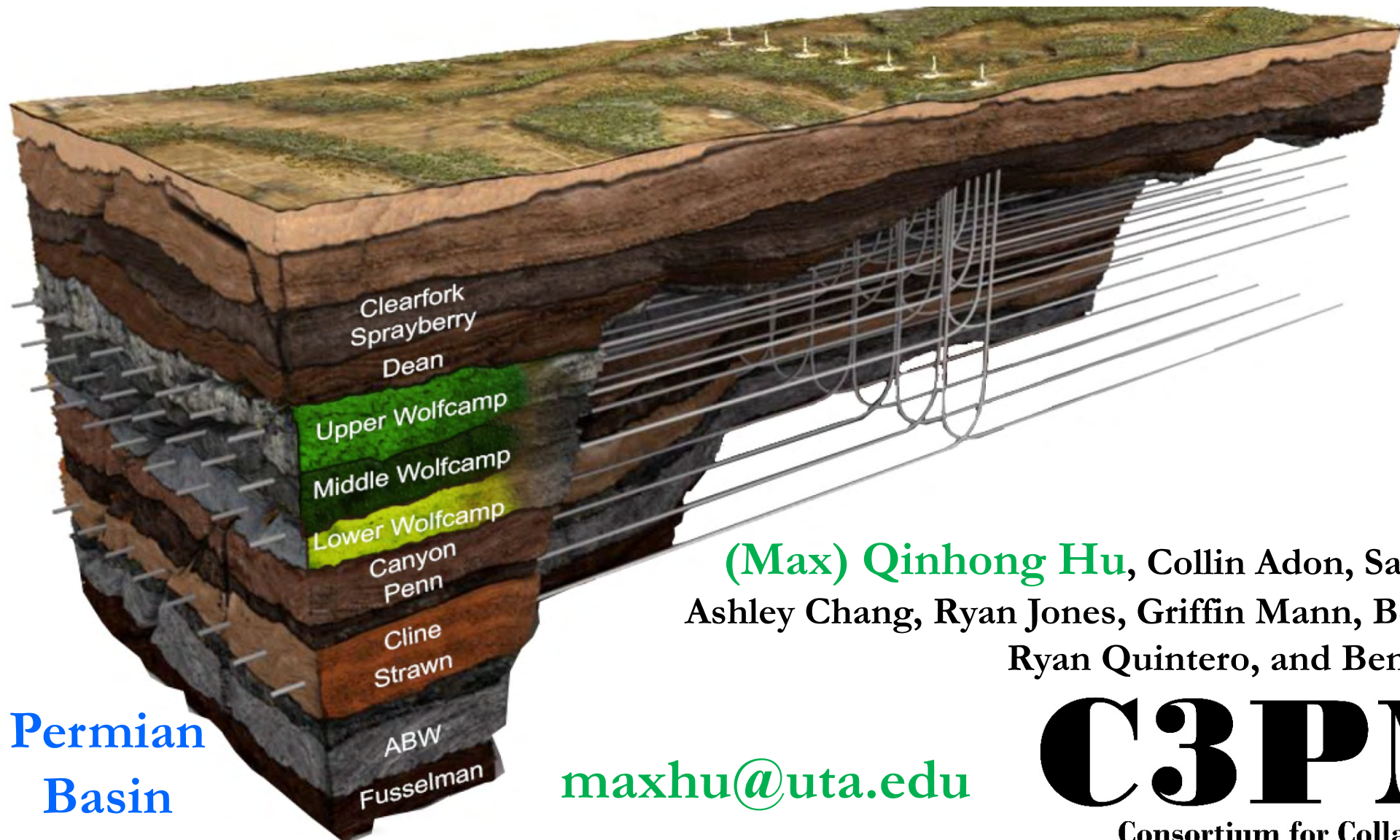
*Adapted from oral presentation accepted for the 2020 AAPG Annual Convention and Exhibition online meeting, September 29 – October 1, 2020.

**Datapages © 2020. Serial rights given by author. For all other rights contact author directly. DOI:10.1306/51688Hu2020

¹University of Texas at Arlington, Arlington, TX, United States (maxhu@uta.edu)

Abstract

The Permian Basin, including Delaware and Midland Basins, has been producing the tightest oil over the past several years. The research on nano-petrophysics, namely the study of rock properties, fluid (gas, liquid hydrocarbon, and formation water) properties, and the rock-fluid interactions within mudrocks with a predominant presence of nano-sized pore space, has been receiving much attention because of its implication in the steep initial decline and low overall recovery of hydrocarbon production from the mudrocks. This study work with a range of mudrocks in both Delaware and Midland Basins with a disparate difference in the geological characteristics. This presentation discusses various approaches to nano-petrophysical studies of the mudrocks, including pycnometry (liquid and gas), pore and bulk volume measurement after vacuum saturation, porosimetry (mercury injection capillary pressure, low-pressure gas physisorption isotherm, nuclear magnetic resonance cyroporometry), imaging (field emission-scanning electron microscopy), tomography (CT, focus ion beam-scanning electron microscopy), small-angle neutron scattering, and the utility of both hydrophilic and hydrophobic fluids as well as fluid invasion tests (imbibition, diffusion, vacuum saturation) followed by laser ablation-inductively coupled plasma-mass spectrometry imaging of different nm-sized tracers. Overall findings indicate that the unique characteristics of low pore connectivity and Dalmatian wettability, further implicated by the entanglement of nano-sized molecules in nanopore space, of these mudrocks, which could lead to a limited matrix-feeding of hydrocarbons to the stimulated fracture network and producing wellbore.



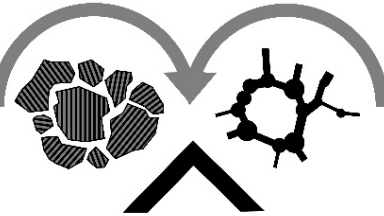
Permian
Basin

maxhu@uta.edu

Nano-Petrophysical Studies of Avalon- Bone Spring- Wolfcamp and Dean-Sprayberry- Wolfcamp Shale Systems

(Max) Qinrong Hu, Collin Adon, Sam Becker, Jordan Bevers,
Ashley Chang, Ryan Jones, Griffin Mann, Benton Mowrey, Nabil Mzee,
Ryan Quintero, and Ben Rogers

C3PM
Consortium for Collaborative
Characterization of Porous Media



$\phi_a \chi \tau r k D$

My Interactions with Stephen Ruppel

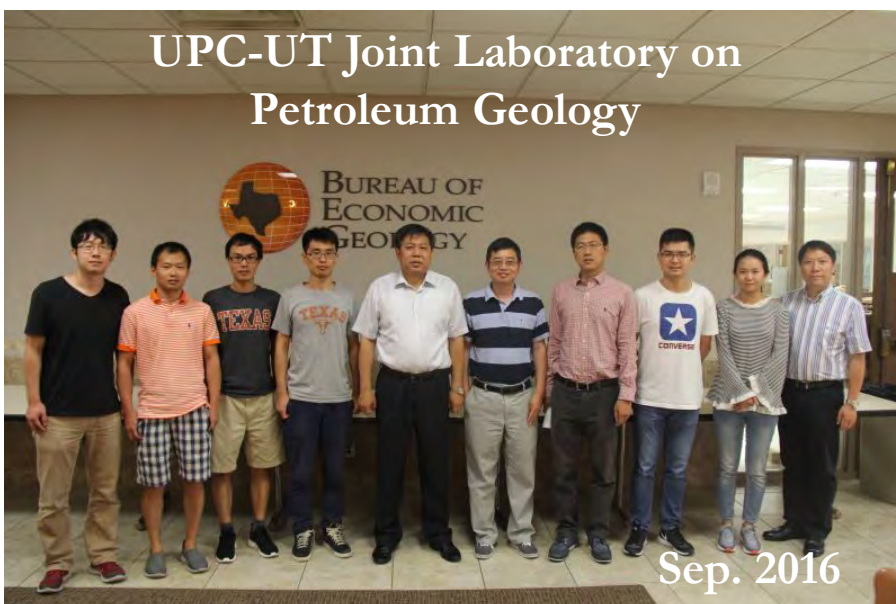
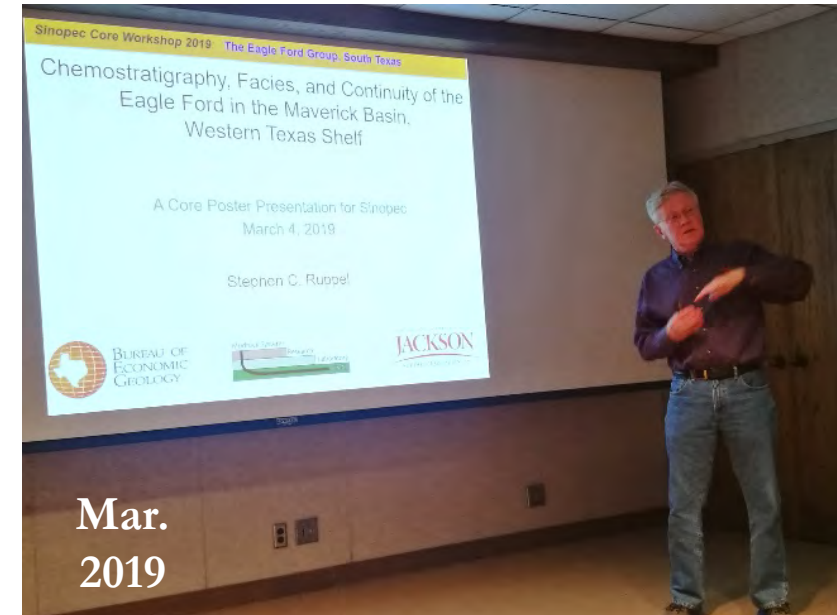


Multiple Approaches to Studying Pore Connectivity

- Imbibition with samples of different shapes
- Edge-only accessible porosity from tracer distribution after vacuum saturation
- Gas diffusion
- Mercury injection porosimeter (down to 3 nm)
- SEM imaging after injection of Wood's metal
- Hysteresis of BET N₂ adsorption/desorption
- Synchrotron microtomography: (ALS @ 1,500 nm ; SLS @ 200 nm)
- Dual Focused Ion Beam (FIB)/SEM nm-scale imaging (EMSL-PNNL)
- Pore-scale network modeling



Dec. 2010 Hedberg



DOE RPSEA shale project (1/2010-2/2014)

Sinopec Short Course 2019: Formation and Characterization of Mudrocks

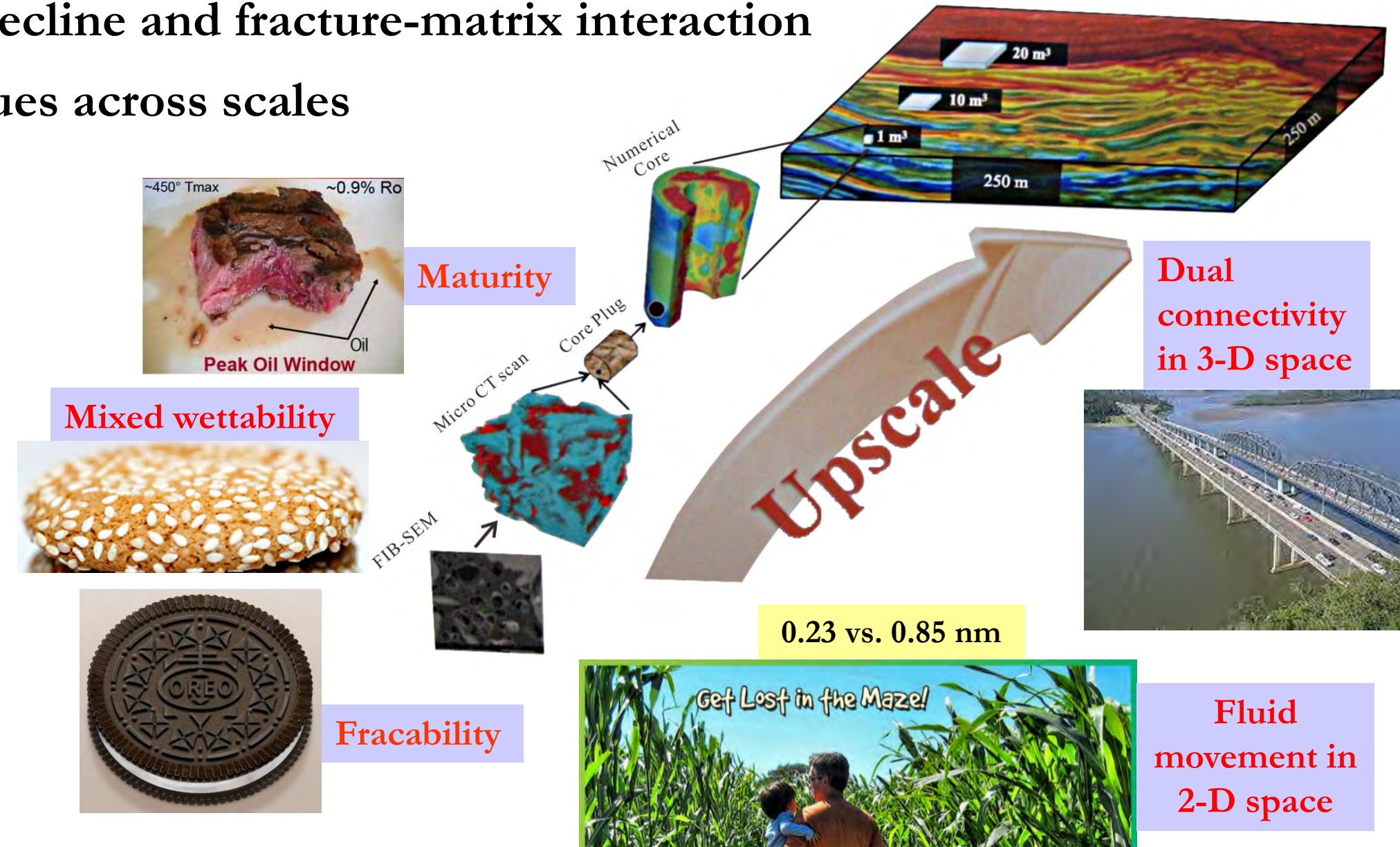
Petrophysics → Nano-Petrophysics

- Petrophysics (*petro* is Latin for "rock" and *physics* is the study of nature)
- The study of properties, as well as interactions, of rock and fluid (gas, liquid hydrocarbons, and aqueous solutions)
- Milestones: Kozeny (1927); Schlumberger brothers (1936); Buckley and Leveret (1941); Archie (1942); 1947: Morse et al. (1947); **Archie (1950; suggested the name of petrophysics)**; Welge (1952); Johnson et al. (1958); 1960s (peak days);

Nano-Petrophysics: petrophysical studies in tight reservoirs with a predominant presence of nanopores

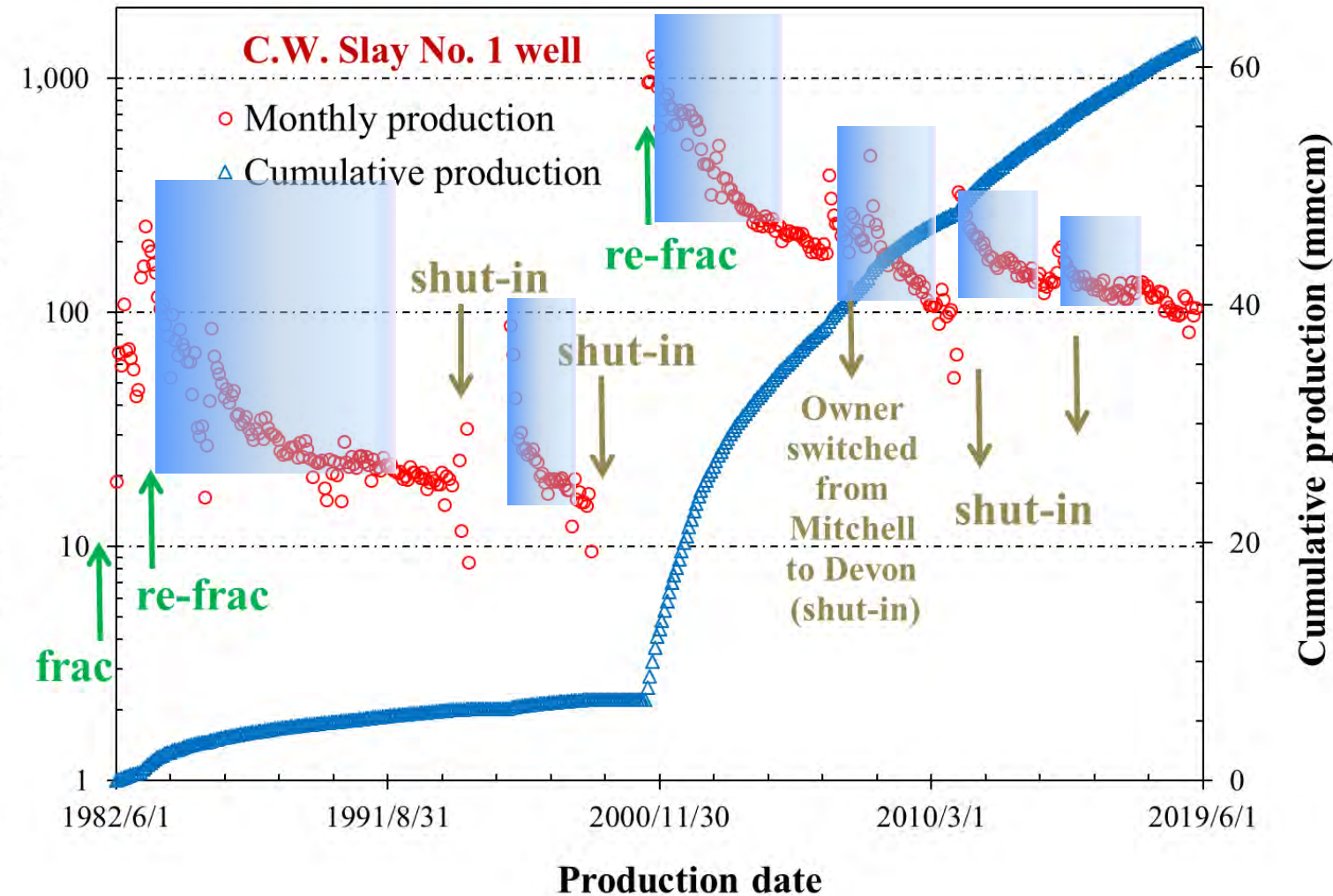
Outline

- Production decline and fracture-matrix interaction
- Scientific issues across scales
 - ✓ Connectivity
 - ✓ Permeability
 - ✓ Capillarity
 - ✓ Wettability
 - ✓ Diffusivity
 - ✓ Tortuosity
 - ✓ Movability
 - ✓ Fracability
 - ✓ Productivity
- Summary

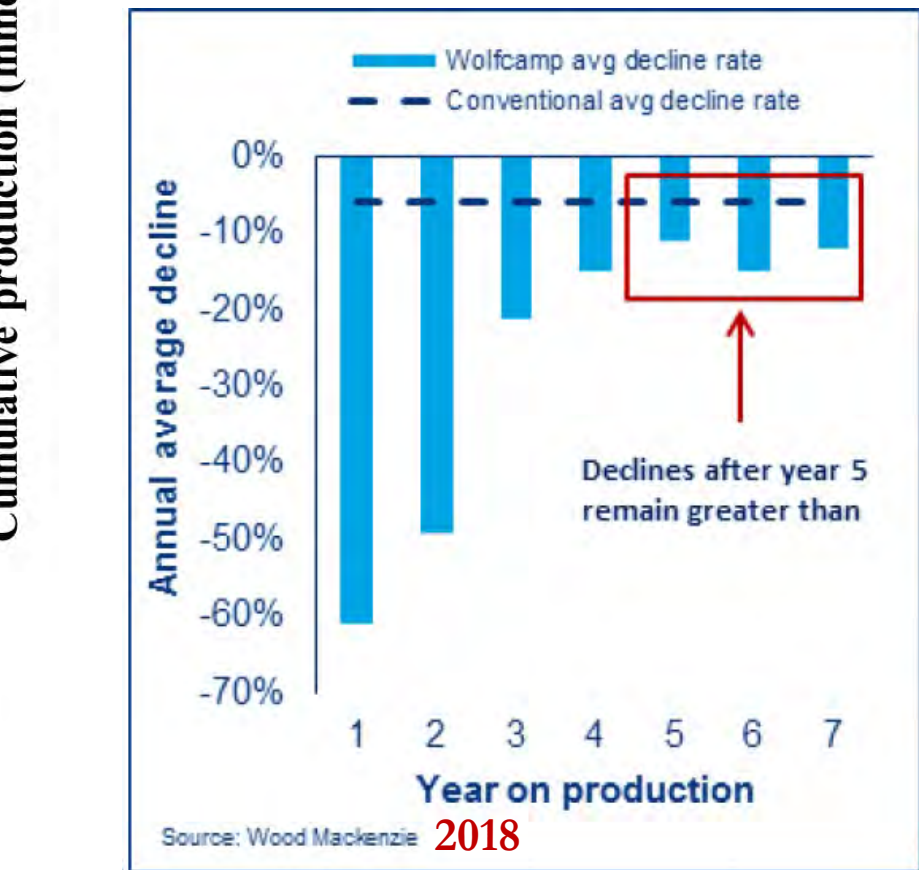


Shale Revolution: Facts

Production history of 1st shale gas well

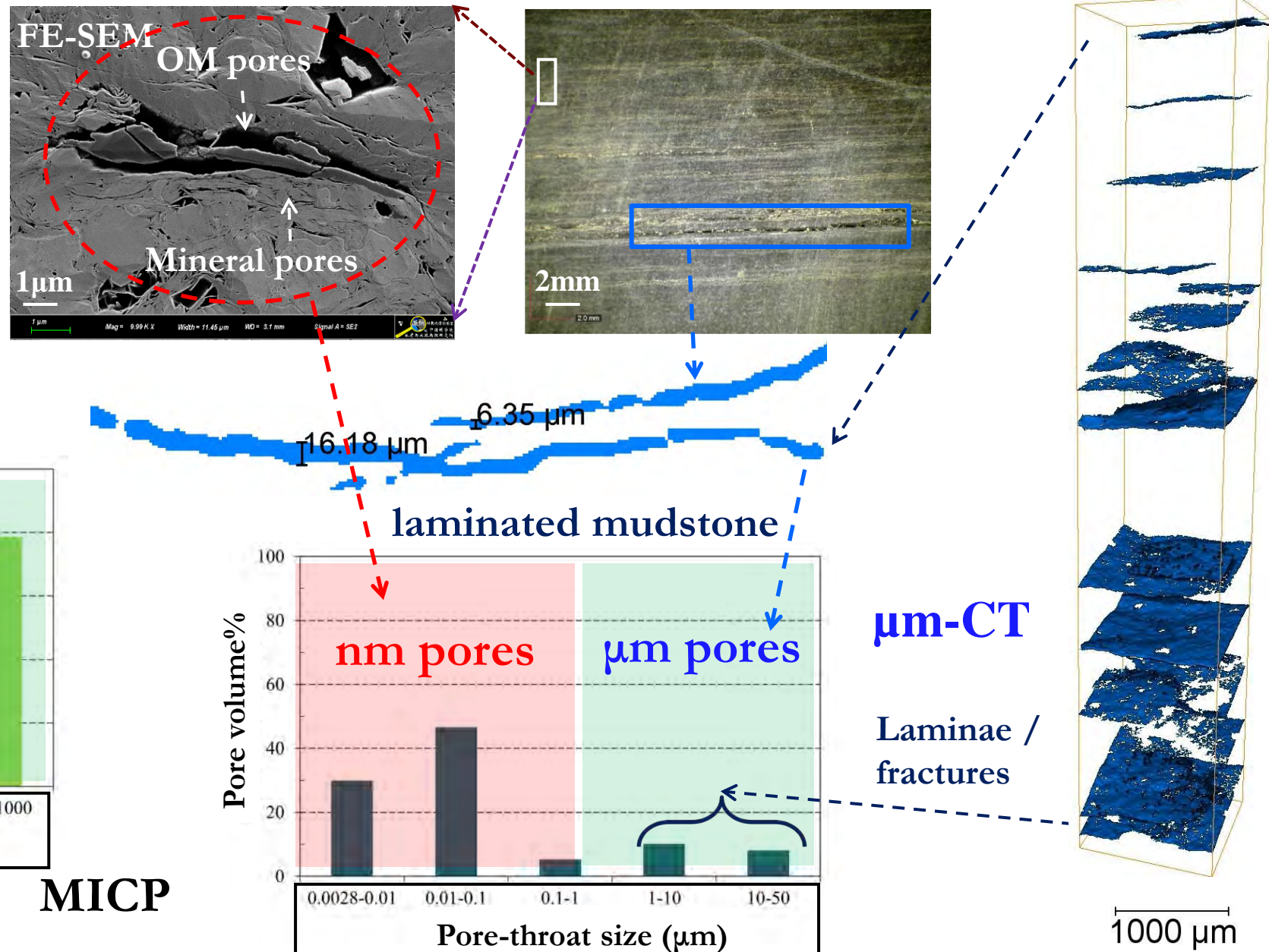


- Steep initial decline (both gas and oil: $\downarrow \frac{2}{3}$ after 1 yr)
- Low recovery (shale gas: <30%; tight oil: <10%)



Conventional vs. Unconventional Reservoirs: Pore Structure

- nm-mm (6 orders of magnitude) pore-fracture systems
- Various pore types of co-existing OM- and minerals-hosted pores
- Unknown pore connectivity with limited methodologies

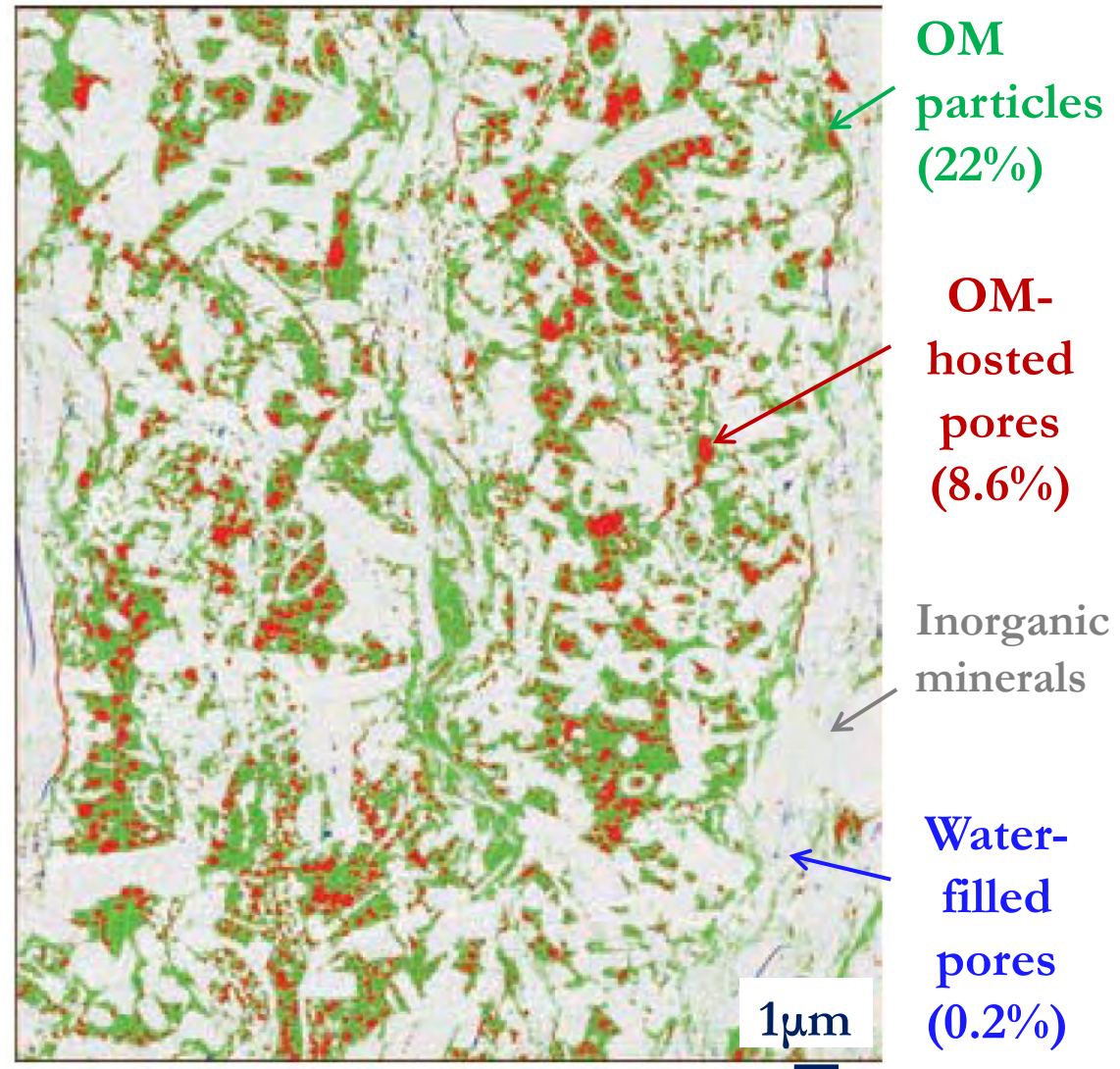
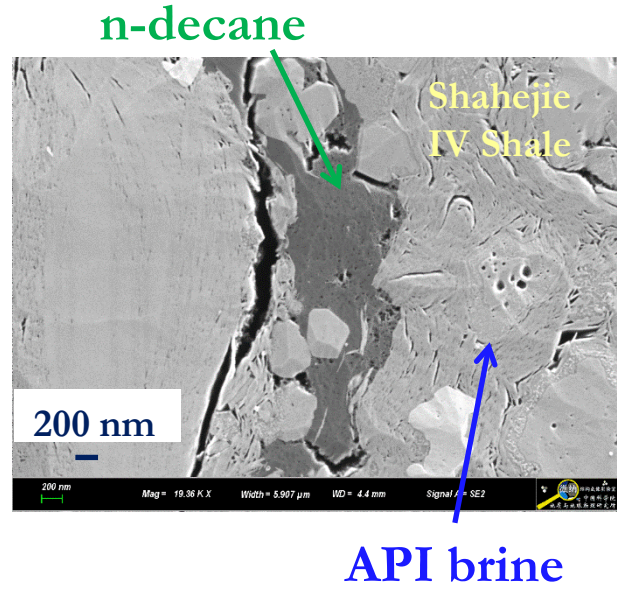


Mudrocks: Mixed Wettability and Associated Pore Structure

- Dalmatian wettability behavior variable at μm scale
- Unknown size, ratio, and connectivity of oil- vs. water-wet pores

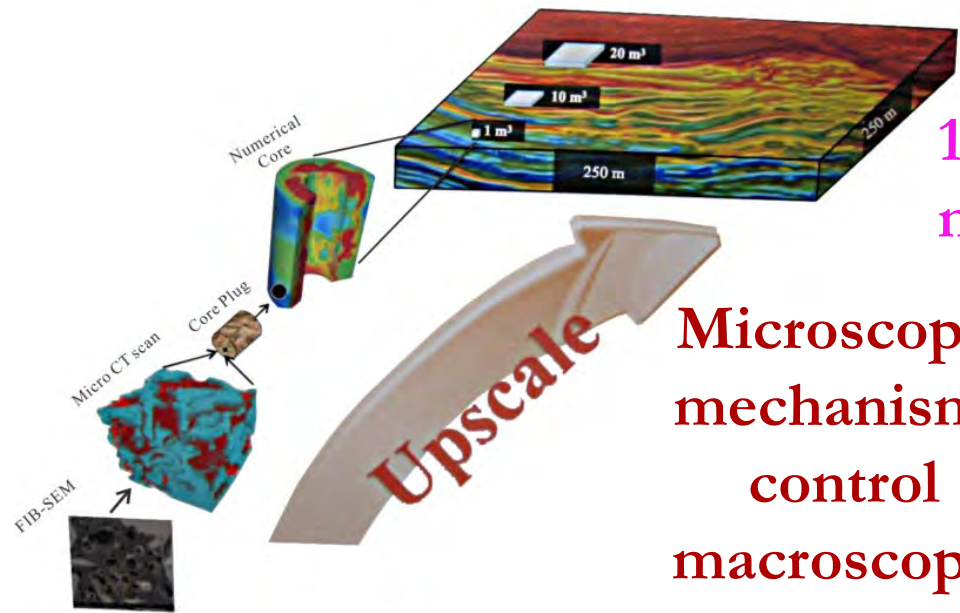


Fluid spreading behavior in a typical mudrock



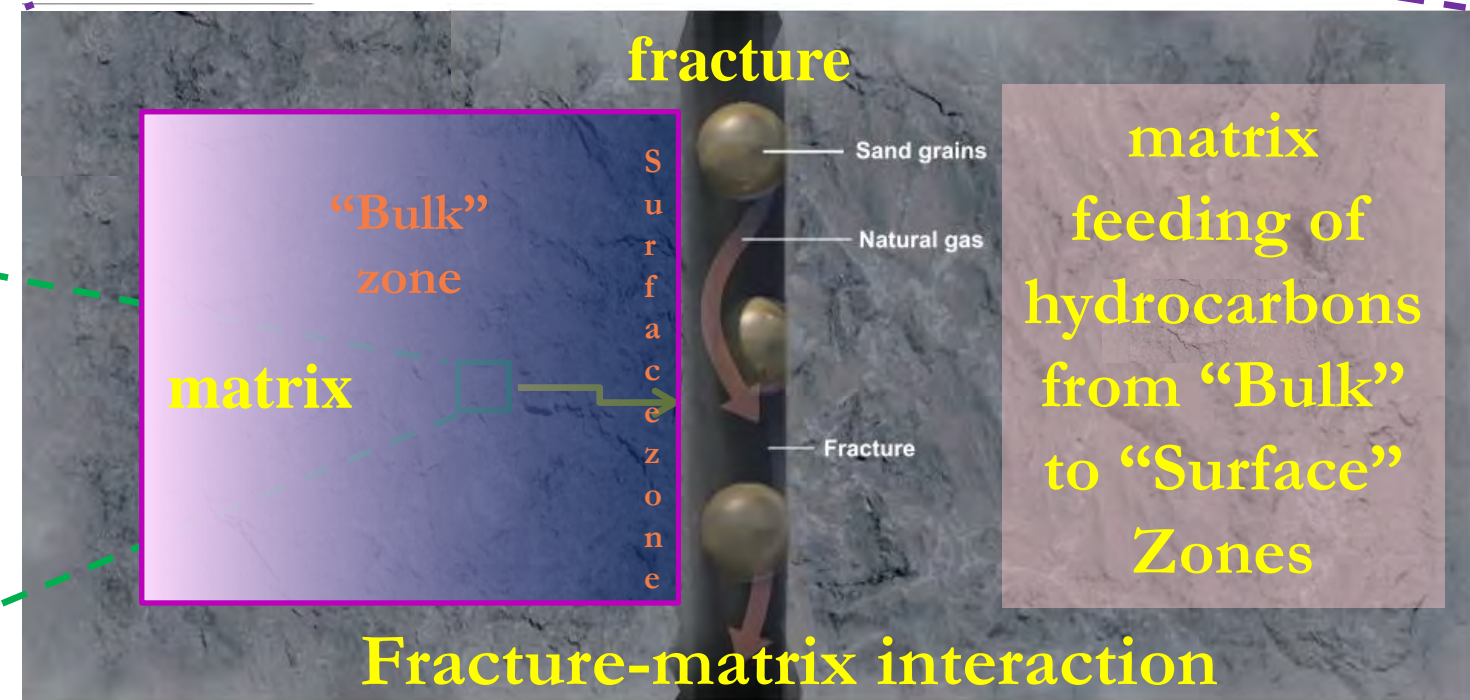
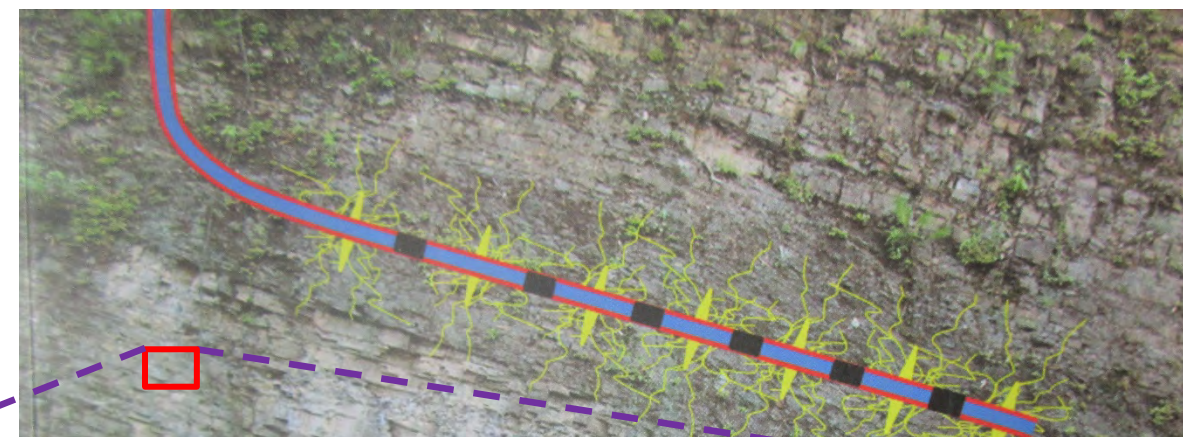
Wolfcamp: SEM (Walls et al., 2016)

Hypothesis: Fracture-matrix Interactions Control Production Behavior in Stimulated mudrock



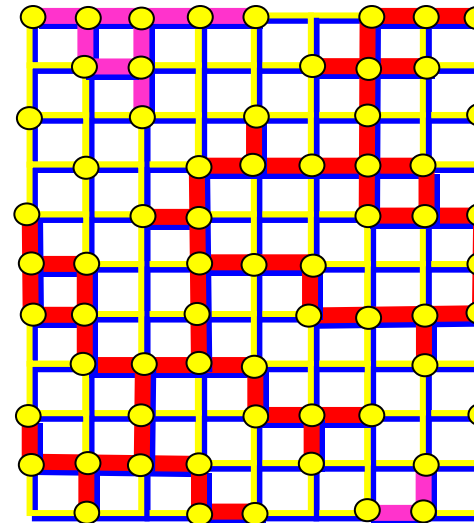
10+ orders of magnitude in scale

Microscopic mechanisms control macroscopic production

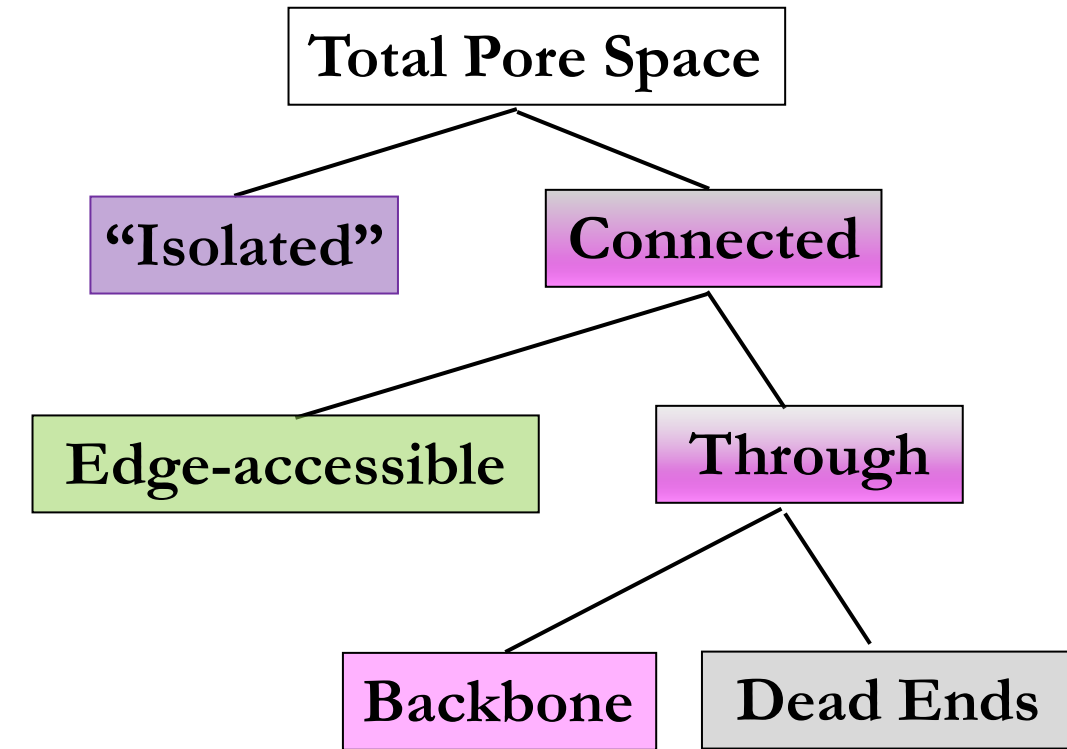


Pore Structure: Geometry and Topology

Percolation theory: the mathematics of how macroscopic properties emerge from local (microscopic) connections



“Surface Zone”: ~400 μm



for mudrock

Effective porosity/Total porosity (ϕ_e/ϕ)

“Surface Zone”: ~70%

“Bulk Zone”: ~0.1%

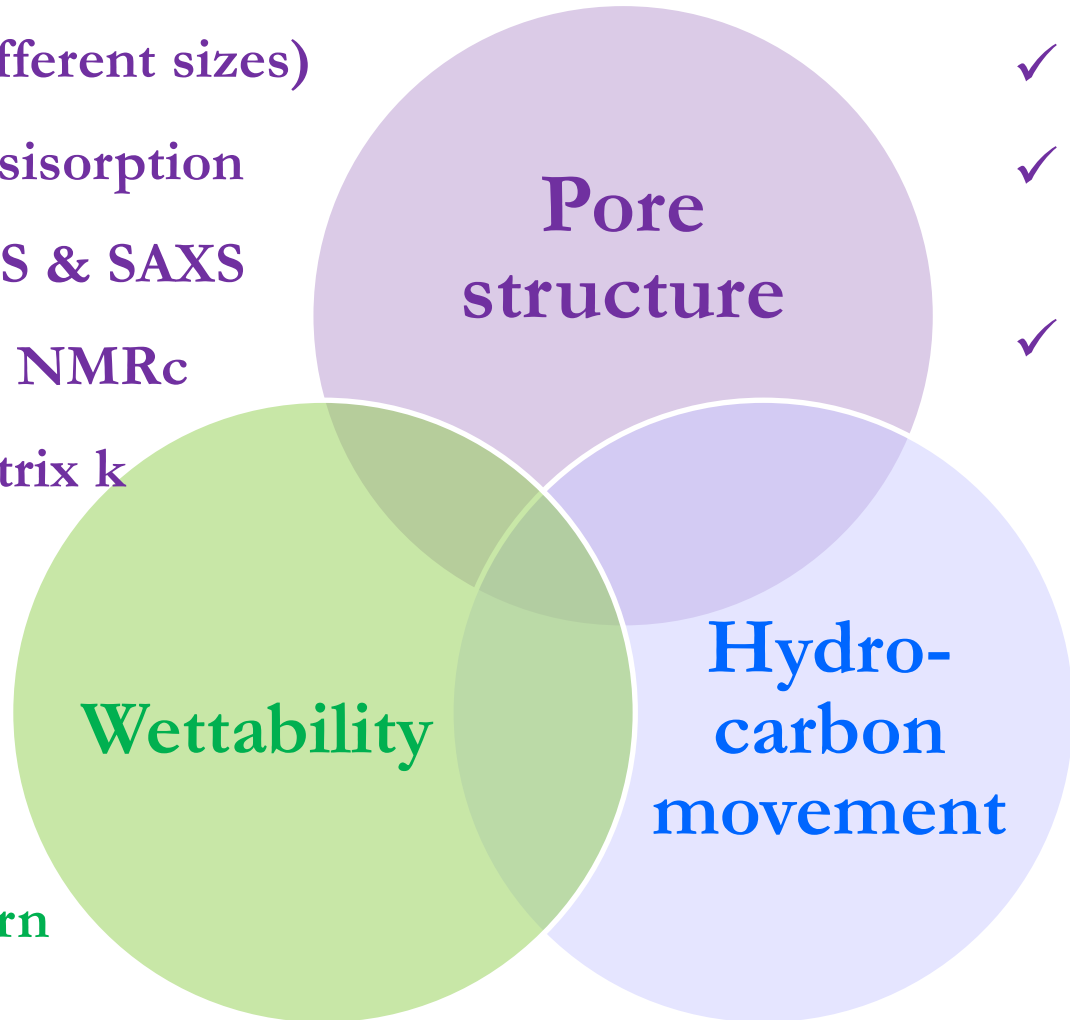
Multi-Approach Nano-Petrophysical Studies

Basic data

- TOC
- Maturity
- Mineralogy
- Pyrolysis
- Thin section
- Well logging
- Production

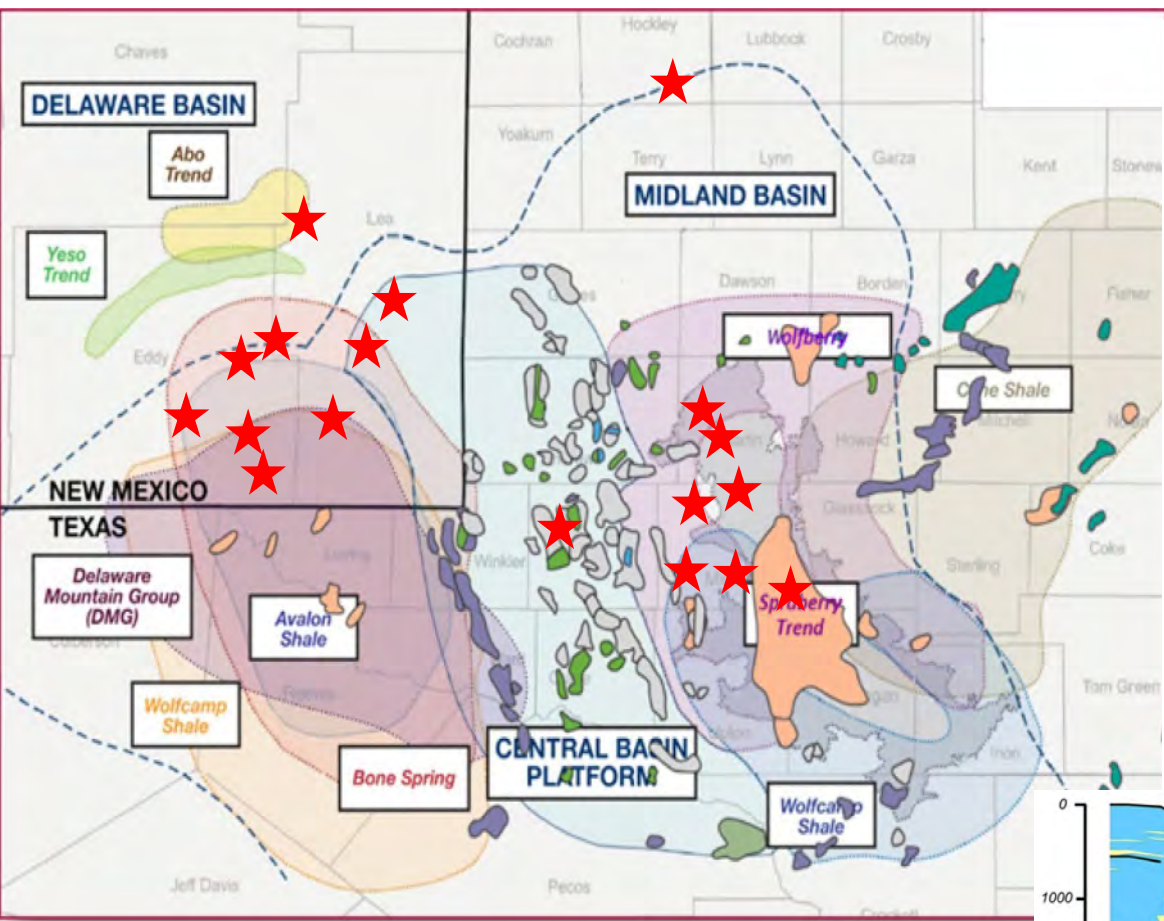
- ✓ Gas and liquid pycnometry
(different sample sizes)
- ✓ MIP (different sizes)
- ✓ Gas physisorption
- ✓ (U)SANS & SAXS
- ✓ NMR & NMRC
- ✓ GRI matrix k

- ✓ Contact angle
- ✓ Imbibition
- ✓ QEMSCAN for Dalmatian pattern

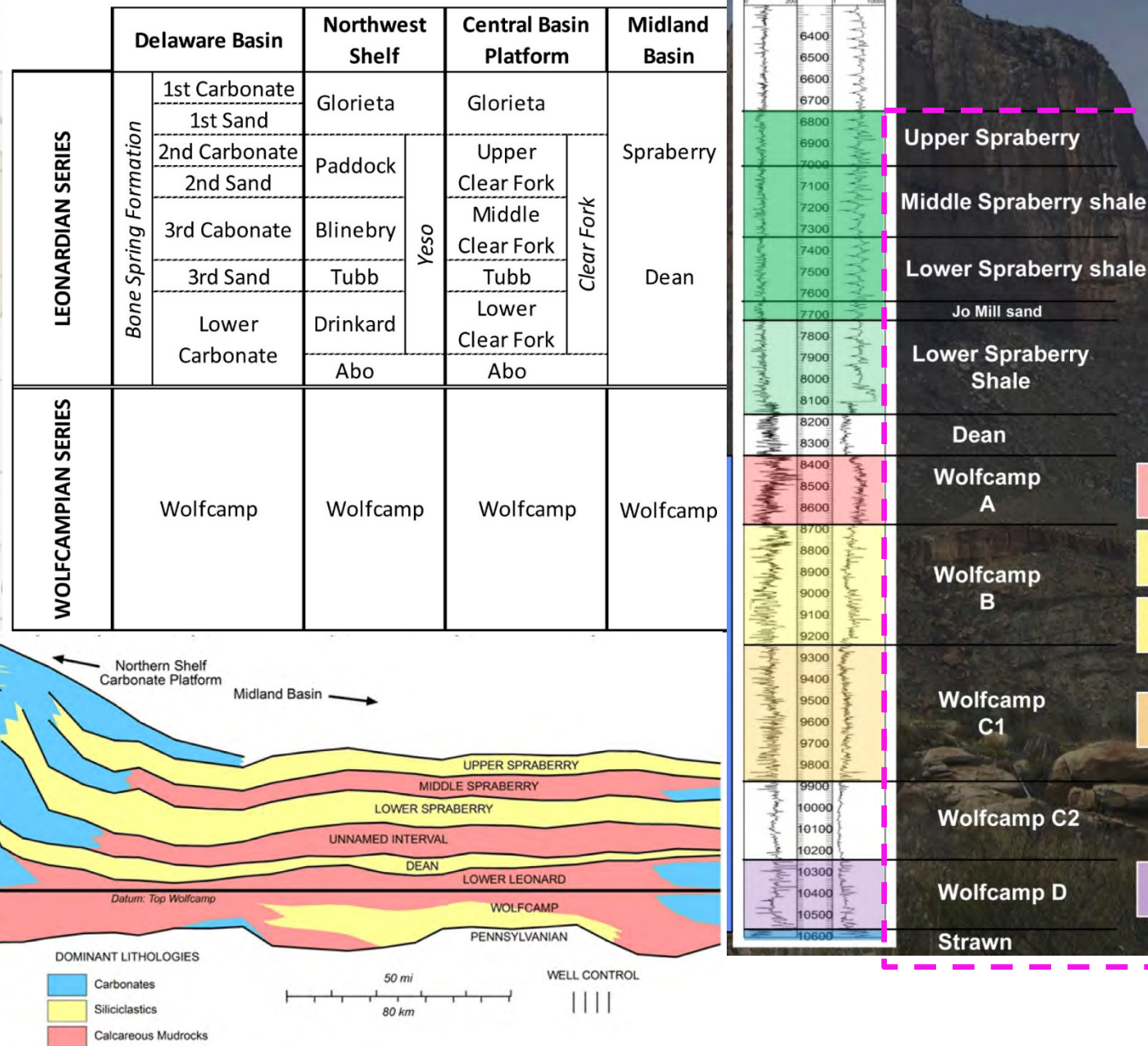


- ✓ FE-SEM & FIB-SEM
- ✓ μm & nm CT
- ✓ Wood's metal impregnation
- ✓ Vacuum saturation & high-pressure intrusion
- ✓ Imbibition
- ✓ Wettability tracers
- ✓ Imbibition (HPHT)
- ✓ Diffusion (HPHT)
- ✓ NMR (HPHT)
- ✓ Core & dm-block flooding (HPHT)

Permian Basin



- 86,000 sq. miles (2.26% USA)
- 52 counties



Multiple Sample Sizes for Different Tests



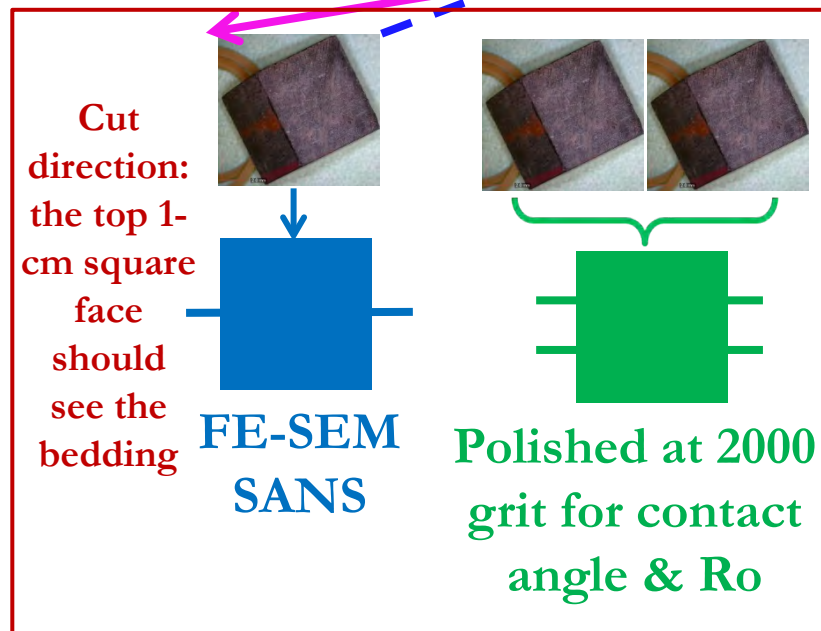
(3) Crush ALL fragments into 6 different size fractions



(2) 3 pieces @2-3 cm for thin section, SANS / SAXS wafer, and backup; 5 mm cubes; 4 mm dia. cylinders

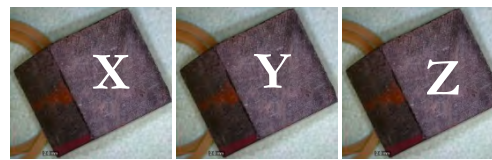


(2) Cut up to 14 1-cm sized cubes

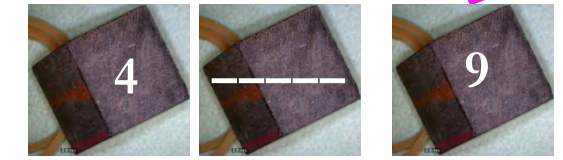


Epoxyed for imbibition

Upward imbibition direction: parallel to bedding



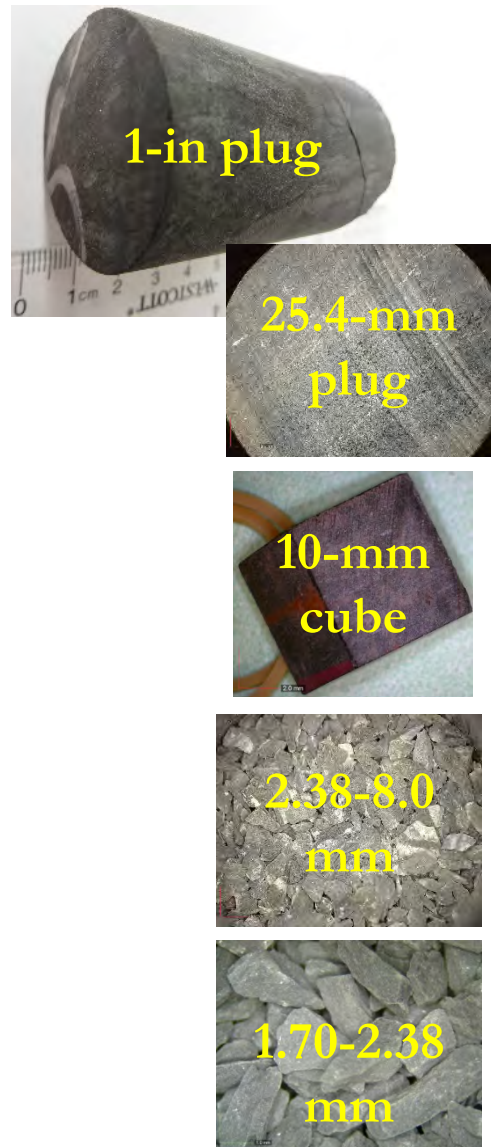
Vac sat (DIW)
↓
MIP
Vac sat (2DT)
Vac sat (DMF)



Tracers-containing tests of vacuum saturation, imbibition, diffusion (possible)

Save into a glass vial for solvent extraction

Multiple Sample Sizes: Plug, Cube, and Grains

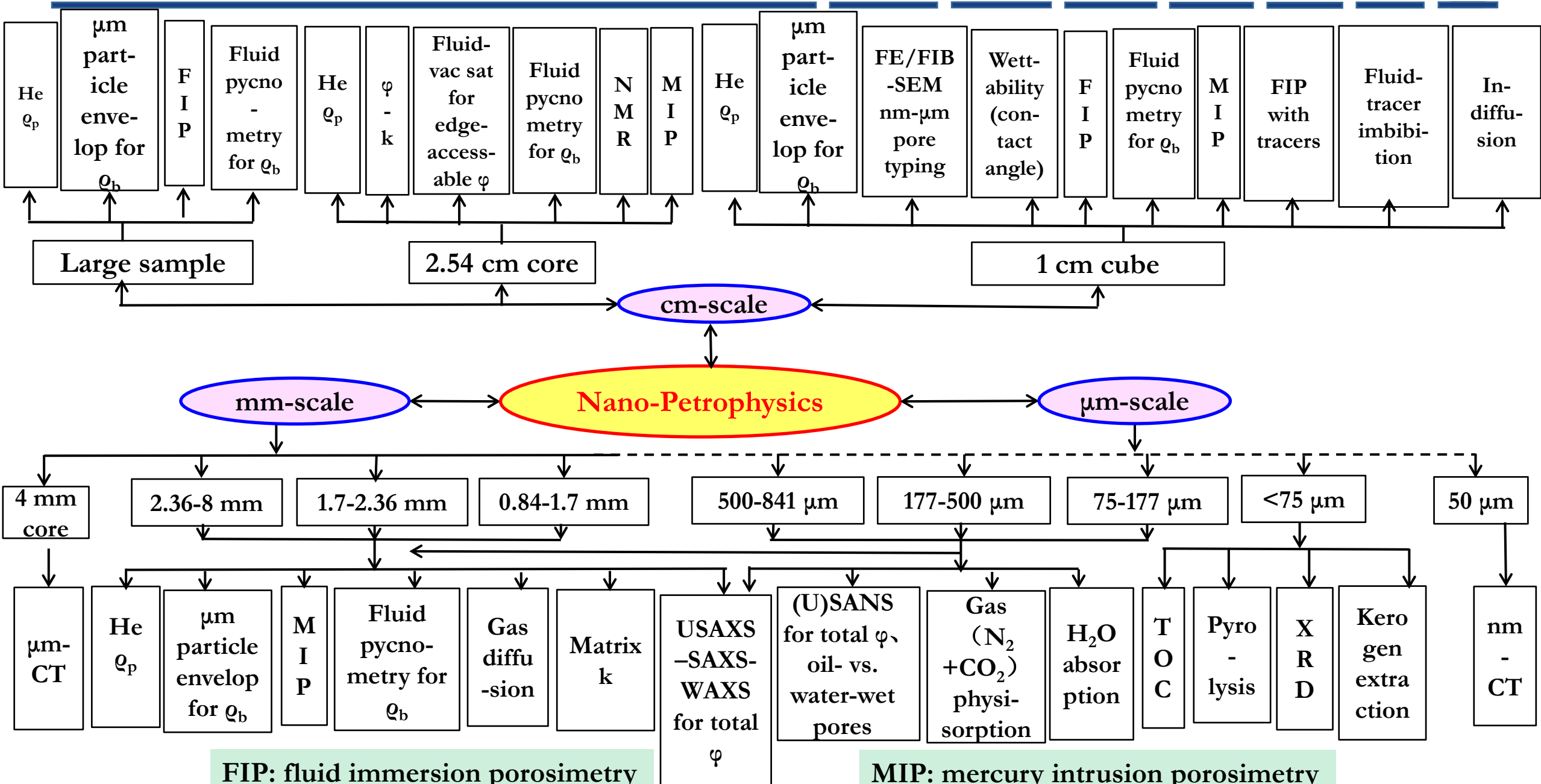


Size designation	Sieve mesh	Size fraction (diameter)	Equivalent spherical dia. (μm)	Equivalent spherical dia. (mm)	
Cylinder / Plug		2.54 cm dia.; any height (e.g., 3 cm)	(24394)	(24.39)	0.84-1.70 mm
Cube		1.0 cm	9086	9.086	500-841 μm
Size X	8 mm to #8	2.38 - 8.0 mm	5180	5.180	177-500 μm
GRI+	#8 to #12	1.70 - 2.38 mm	2030	2.030	75-177 μm
Size A	#12 to #20	841 - 1700 μm	1271	1.271	<75 μm
GRI	#20 to #35	500 - 841 μm	671	0.671	
Size B	#35 to #80	177 - 500 μm	339	0.339	
Size C	#80 to #200	75 - 177 μm	126	0.126	
Powder	<#200	< 75 μm	< 75	< 0.075	
Size D	#200 to #625	20 - 75 μm	47.5	0.0475	
Size E	<#635	<20 μm	<20	<0.02	

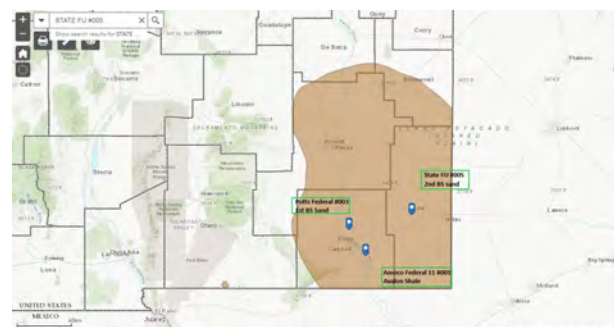
GRI: Gas Research Institute

Overlaps “Surface Zone” and “Bulk Zone” for mudrock

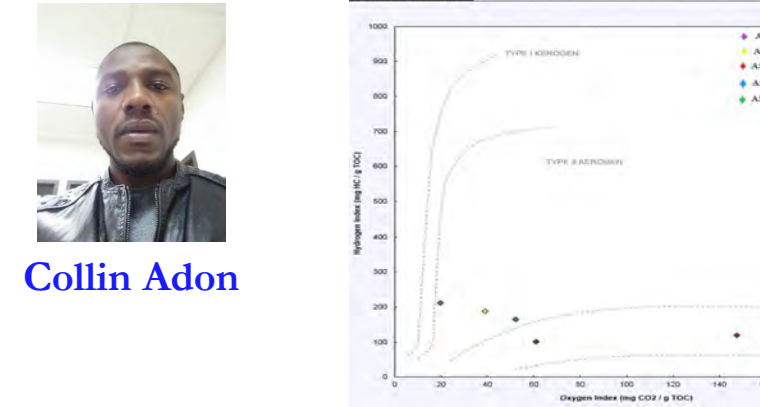
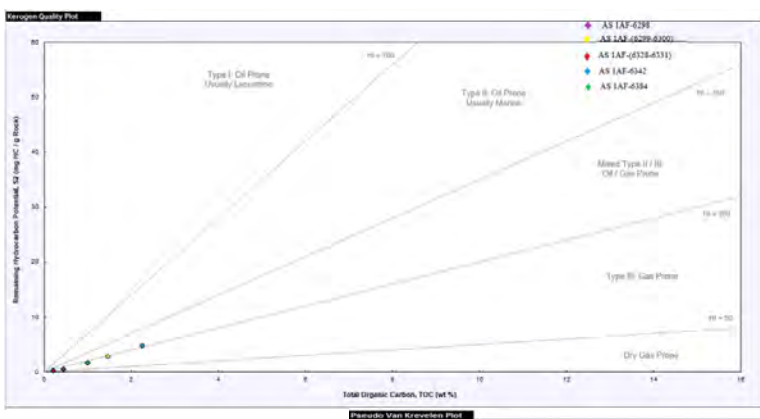
Experiments, Sample Sizes and Research Objectives



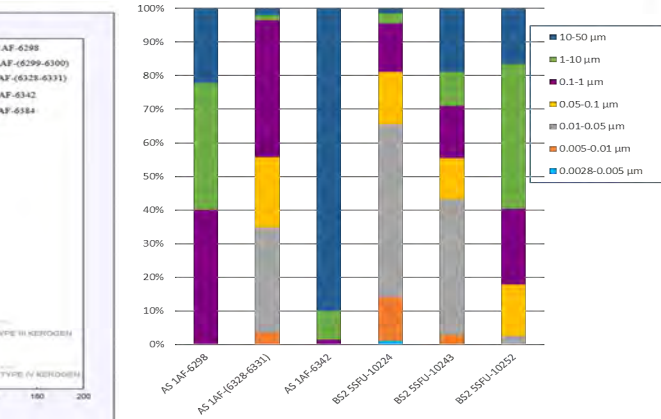
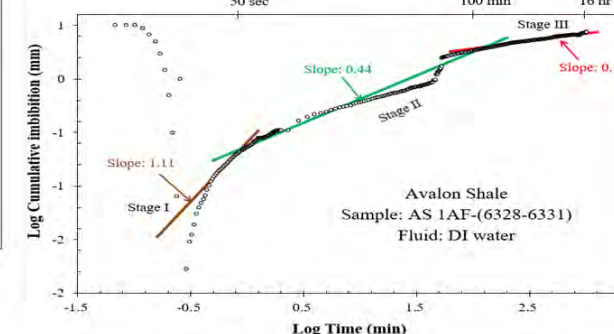
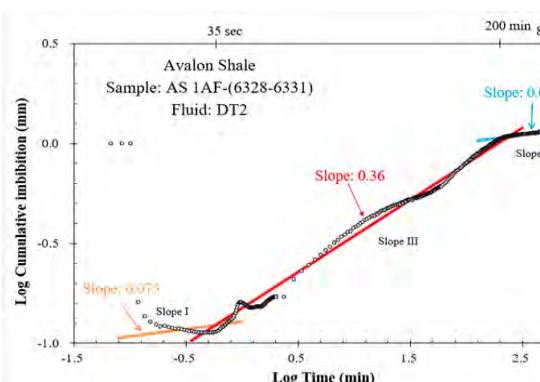
Delaware Basin: Avalon & Bone Spring



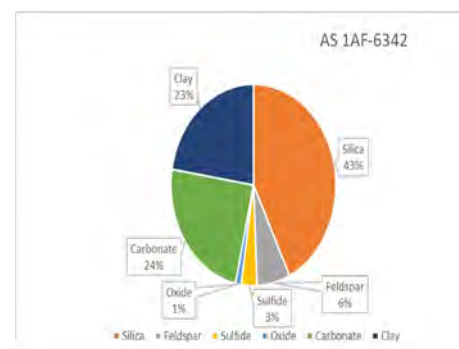
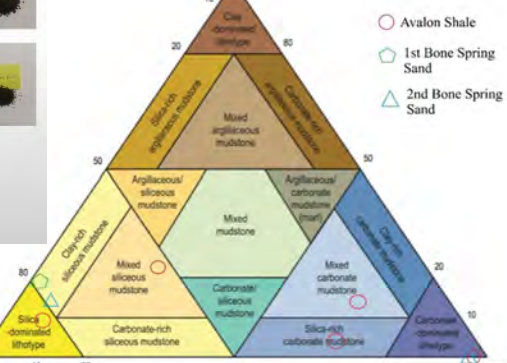
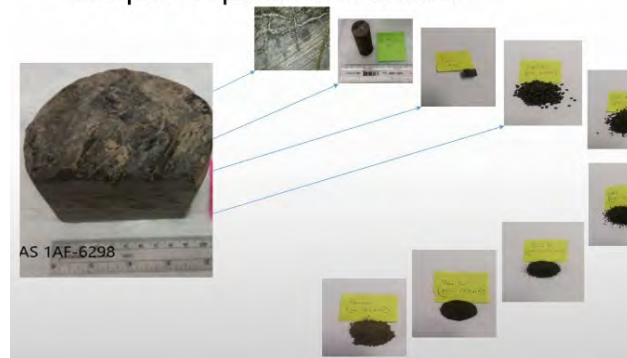
Well No	Formation	Depth (ft.)	sCore Descriptions
1	Avalon Shale	6298	carbonate-dominated lithotype
		6299-6300	mixed carbonate mudstone
		6328-6331	silica-dominated lithotype
		6342	mixed siliceous mudstone
		6384	silica-rich carbonate mudstone
2	First Bone Spring Sand	6257	clay-rich siliceous mudstone
3	Second Bone Spring Sand	10224	clay-rich siliceous mudstone
		10252	carbonate-dominated lithotype



Collin Adon

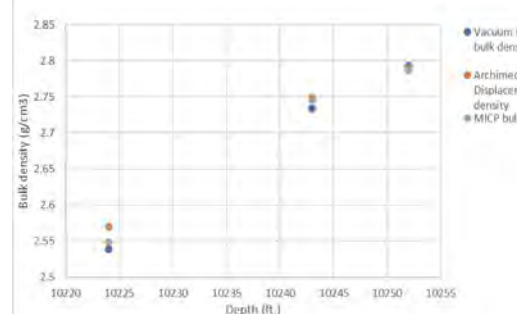


Sample Preparation Workflow



Vacuum Saturation Results

Sample ID	Porosity (%)	Clay		Sand		Volume (ml)
		Bulk Density (g/ml)	Visco Density (g/ml)	Bulk Density (g/ml)	Visco Density (g/ml)	
AS 1AF-6298	4.04	2.000	2.030	3.750	2.031	424.71
AS 1AF-6342	1.03	2.02	2.07	4.20	2.021	120.0
AS 1AF-6331	5.95	3.63	3.64	1.980	2.001	100.1
852.SSPU-10224	3.12	2.60	2.62	—	—	—
852.SSPU-10243	—	—	—	2.760	2.760	—
852.SSPU-10252	—	—	—	2.760	2.760	—



•

- Porosity for Avalon shale range b/w 0.4% to 6.7%, and 0.7% to 3% for the 2nd Bone Spring Sand.
- Result for Avalon shale show no discernible trend.

•

- For cube-sized samples, the 2nd Bone Spring porosity decreases as bulk density & grain density increases

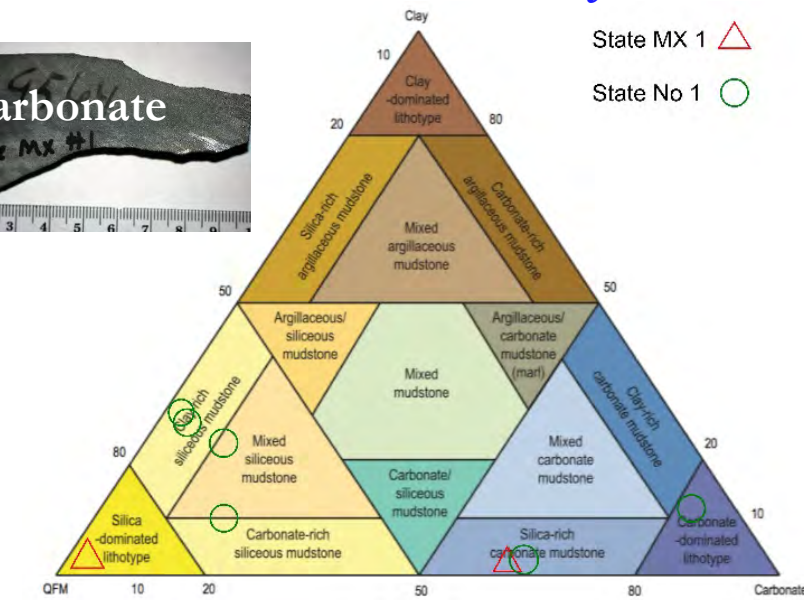
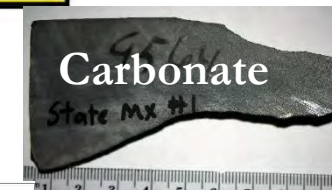
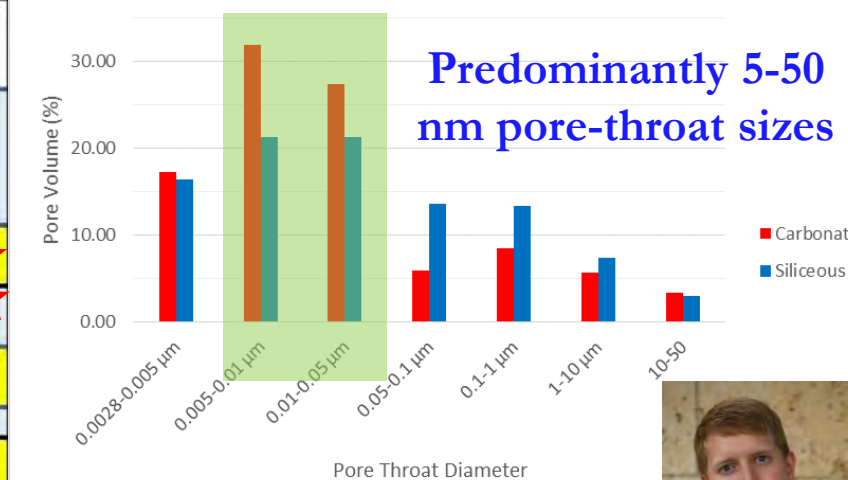
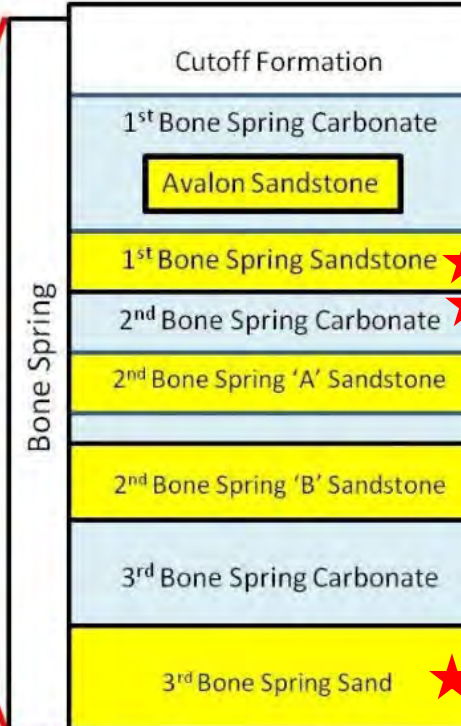
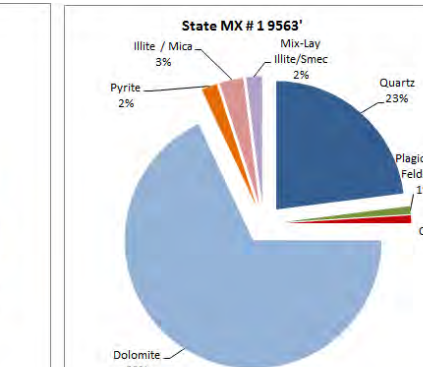
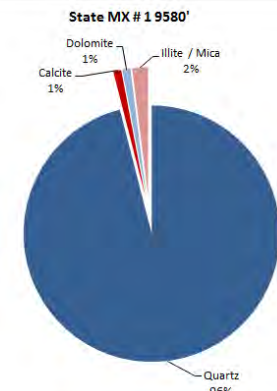
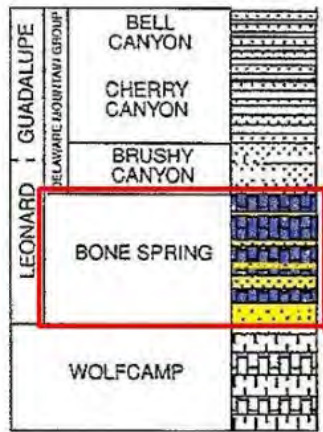
Delaware Basin: Bone Spring-Wolfcamp

System

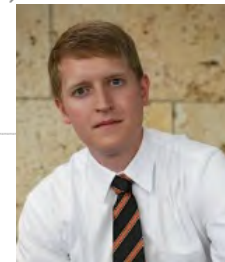
Delaware Basin

Permian

Dewey Lake
Rustler
Salado
Castile
Lamar
Bell Canyon
Cherry Canyon
Brushy Canyon
Avalon Shale
Bone Spring
1st Bone Spring Sand
2nd Bone Spring Sand
3rd Bone Spring Sand
Wolfcamp
Cisco
Canyon
Strawn
Atoka
Morrow



Predominantly 5-50 nm pore-throat sizes



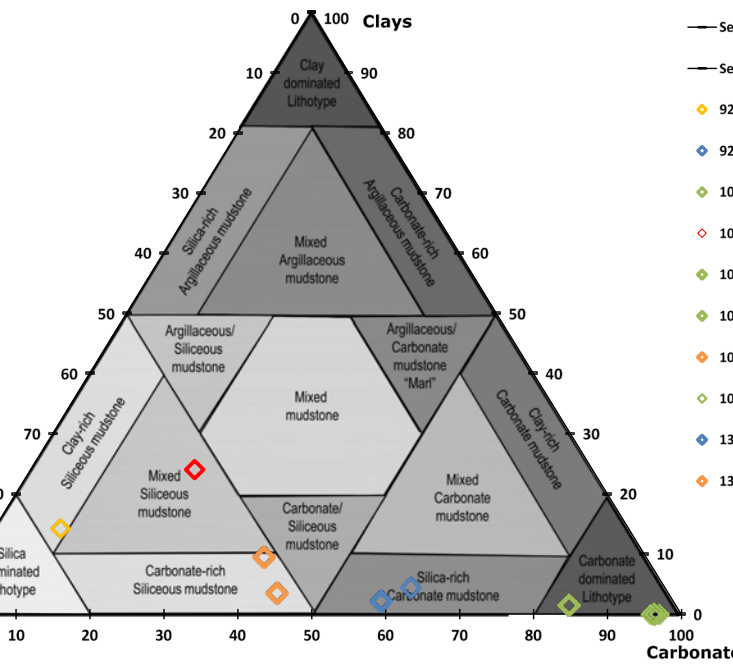
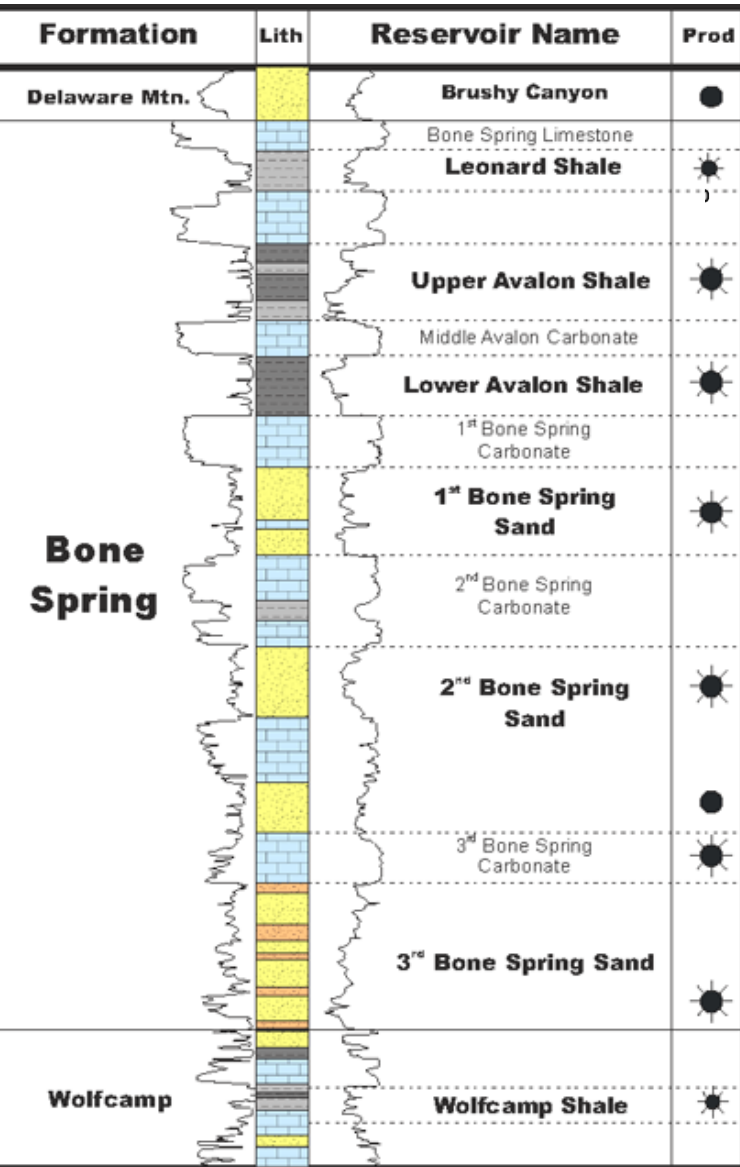
Jordan Bevers

State MX 1 ▲

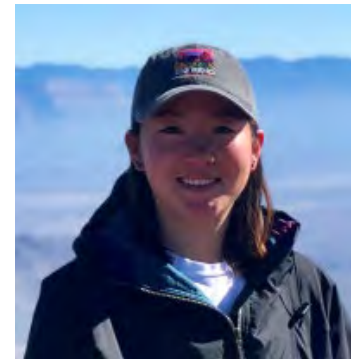
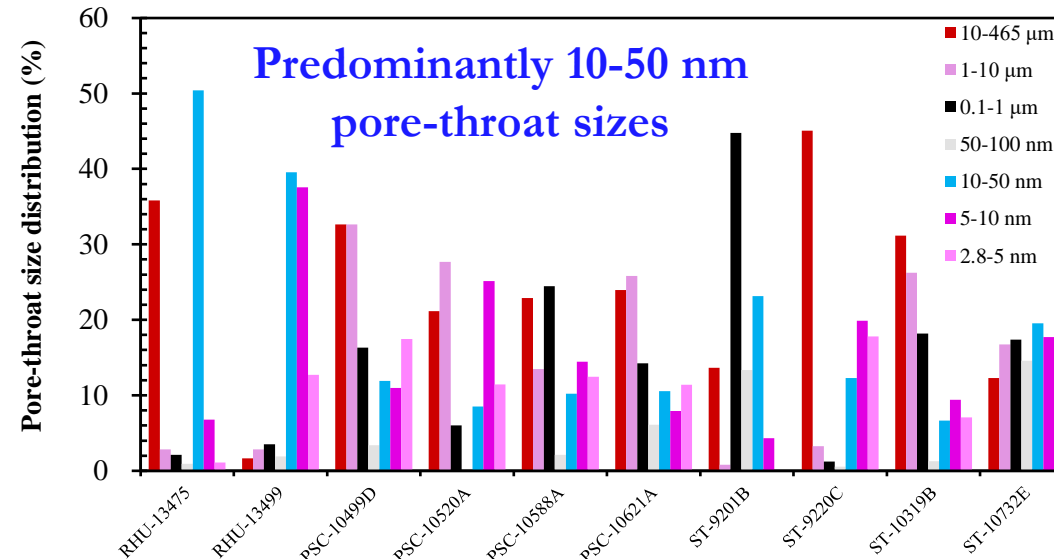
State No 1 ○

Delaware Basin: Bone Spring-Wolfcamp

PERMIAN



Formation	Lithofacies	Vacuum saturation (1 cm cube)	MICP (1 cm cube)
		Porosity (%)	
Wolfcamp	Carbonate dominated lithotype	0.608-3.30	0.360-5.90
	Carbonate-rich siliceous mudstone	0.768-1.42	0.490-2.36
	Mixed Siliceous mudstone	2.83	1.38
	Silica-rich carbonate mudstone	5.38	5.83
First Bone Spring	Clay-rich siliceous mudstone	6.33	6.44
	Silica-rich carbonate mudstone	0.800	5.23
Second Bone Spring	Carbonate dominated lithotype	5.49	7.65



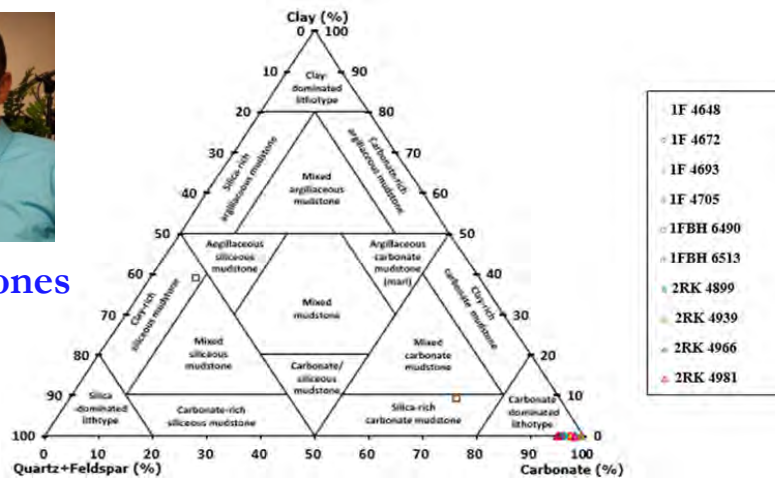
Ashley Chang

Delaware Basin: Wolfcamp A

Delaware Basin		
Period	Epoch	Stage
Permian	Guadalupian	Bell Canyon
		Cherry Canyon
		Brushy Canyon
	Leonardian	Bone Spring Lime
		Avaen Sand
		First Bone Spring
Wolfcampian	Second Bone Spring	Second Bone Spring
		Third Bone Spring
		Wolfcamp A
	Wolfcampian	Wolfcamp B
		Wolfcamp C
		Wolfcamp D
Carboniferous	Pennsylvanian	Strawn
		Atoka

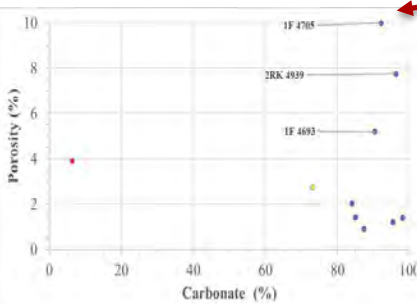


Ryan Jones

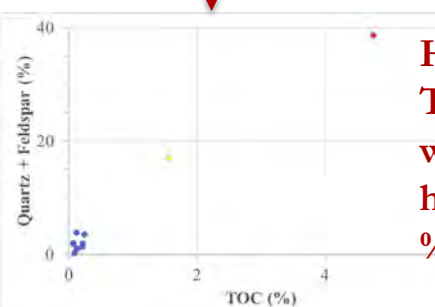


- 1F 4648
- 1F 4672
- 1F 4693
- 1F 4705
- 1FBH 6490
- 1FBH 6513
- 2RK 4899
- 2RK 4939
- 2RK 4966
- 2RK 4981

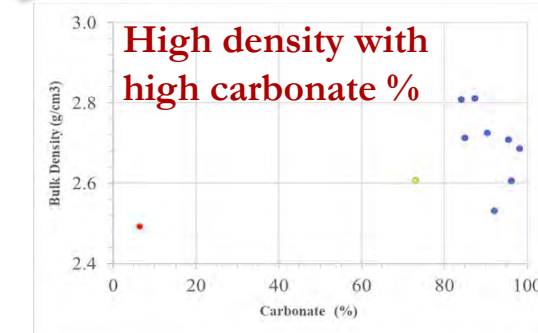
Sample ID	MICP Porosity (%)	Vacuum Saturation Porosity (%)			Average (%)
		DI Water	DT2	THF	
1F 4648	1.004	1.230	1.967	1.436	1.409
1F 4672	N/A	2.309	2.373	1.386	2.023
1F 4693	4.885	5.623	5.705	4.575	5.197
1F 4705	9.745	9.799	10.436	9.937	9.979
1FBH 6490	2.682	3.370	4.377	5.155	3.896
1FBH 6513	N/A	2.531	3.185	2.500	2.739
2RK 4899	0.448	0.869	1.599	0.648	0.891
2RK 4939	7.661	8.673	5.724	8.916	7.744
2RK 4966	N/A	0.985	1.893	0.782	1.220
2RK 4981	0.494	1.317	2.078	1.675	1.391



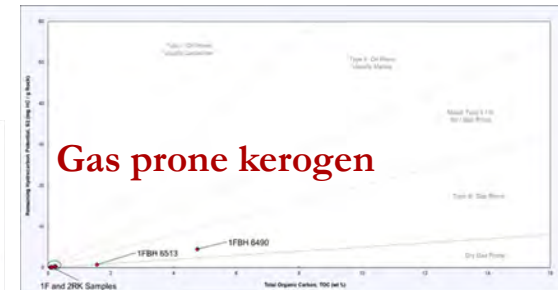
Low porosity with high carbonate %



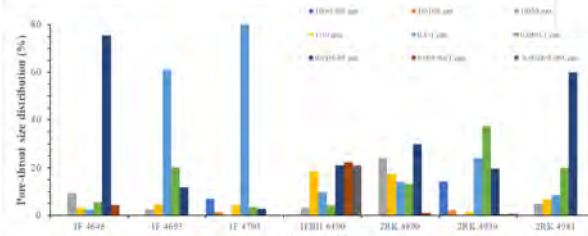
High TOC with high QF %



High density with high carbonate %



Gas prone kerogen

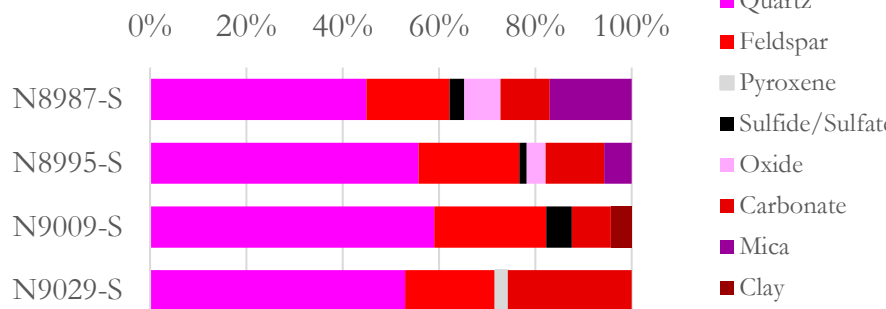
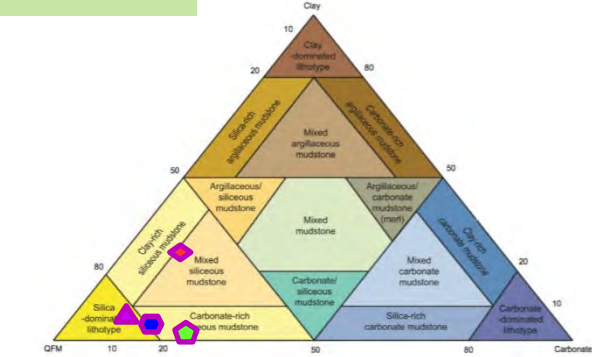
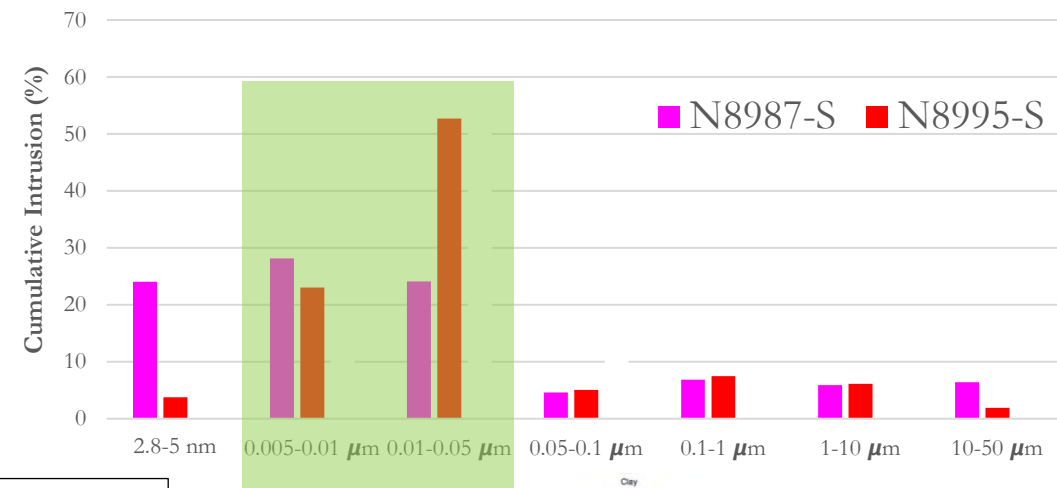
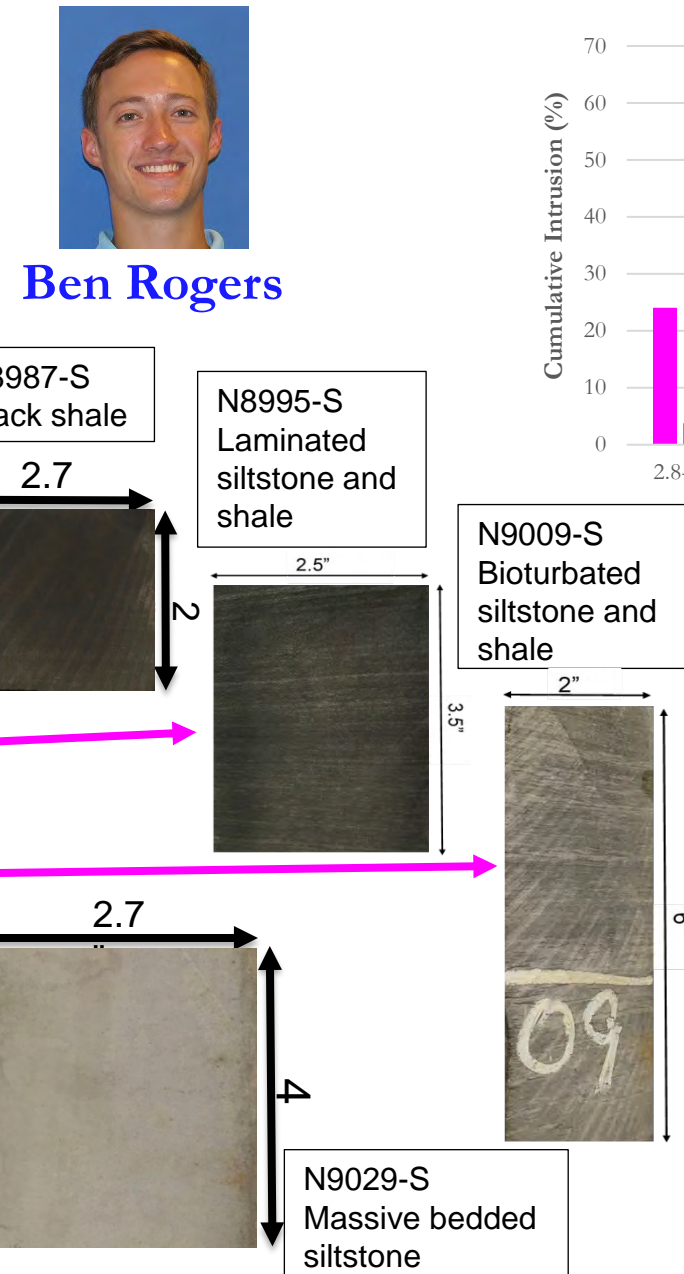
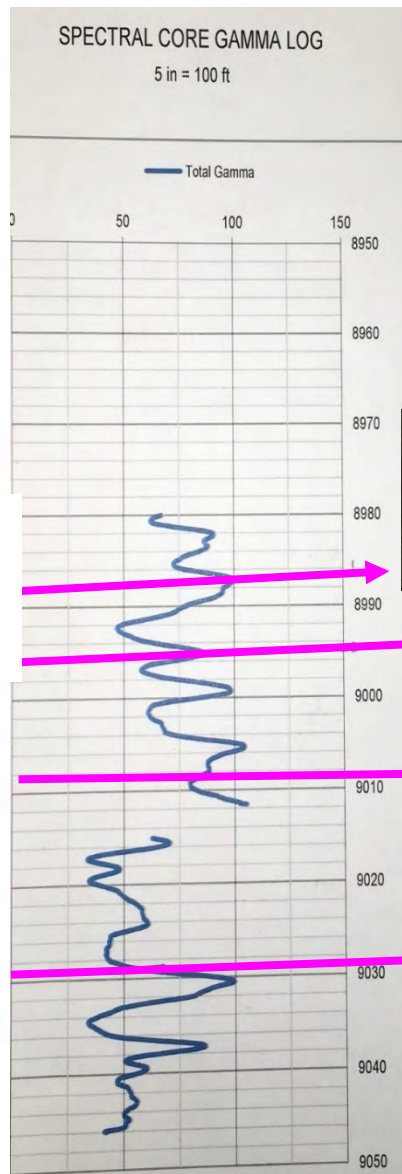
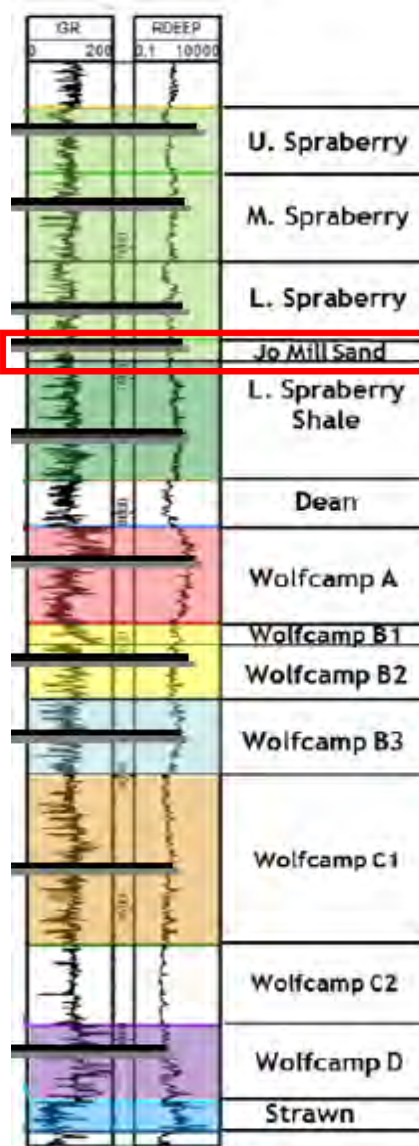


Pore-throat size distribution (MIP)

Intermediate DIW connectivity; High 2DT connectivity

Sample ID	DI Water	Connectivity Classification	DT2	Connectivity Classification
1F 4648	0.274	Intermediate	0.875	High
1F 4672	0.375	Intermediate	0.503	High
1F 4693	0.236	Low	0.700	High
1F 4705	0.330	Intermediate	0.531	High
1FBH 6490	0.628	High	0.848	High
1FBH 6513	0.300	Intermediate	0.330	Intermediate
2RK 4899	0.287	Intermediate	0.652	High
2RK 4939	0.456	Intermediate	0.290	Intermediate
2RK 4966	0.365	Intermediate	N/A	N/A
2RK 4981	0.277	Intermediate	0.512	High

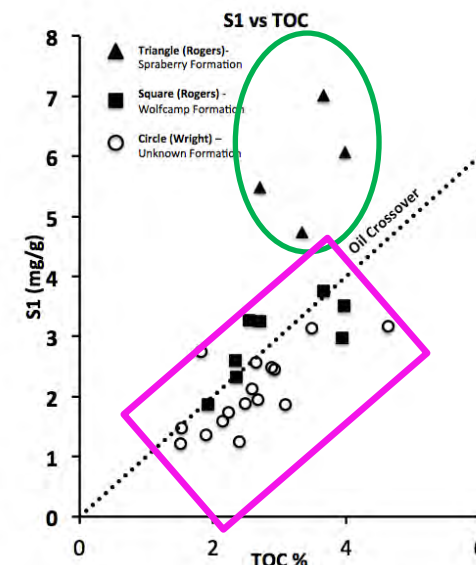
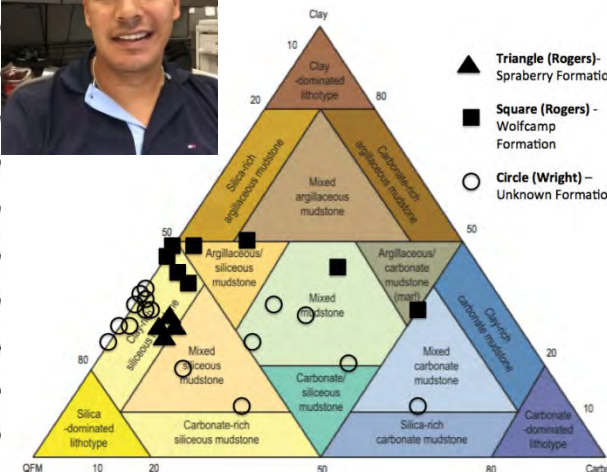
Midland Basin: Jo Mill Submarine Fan Complex



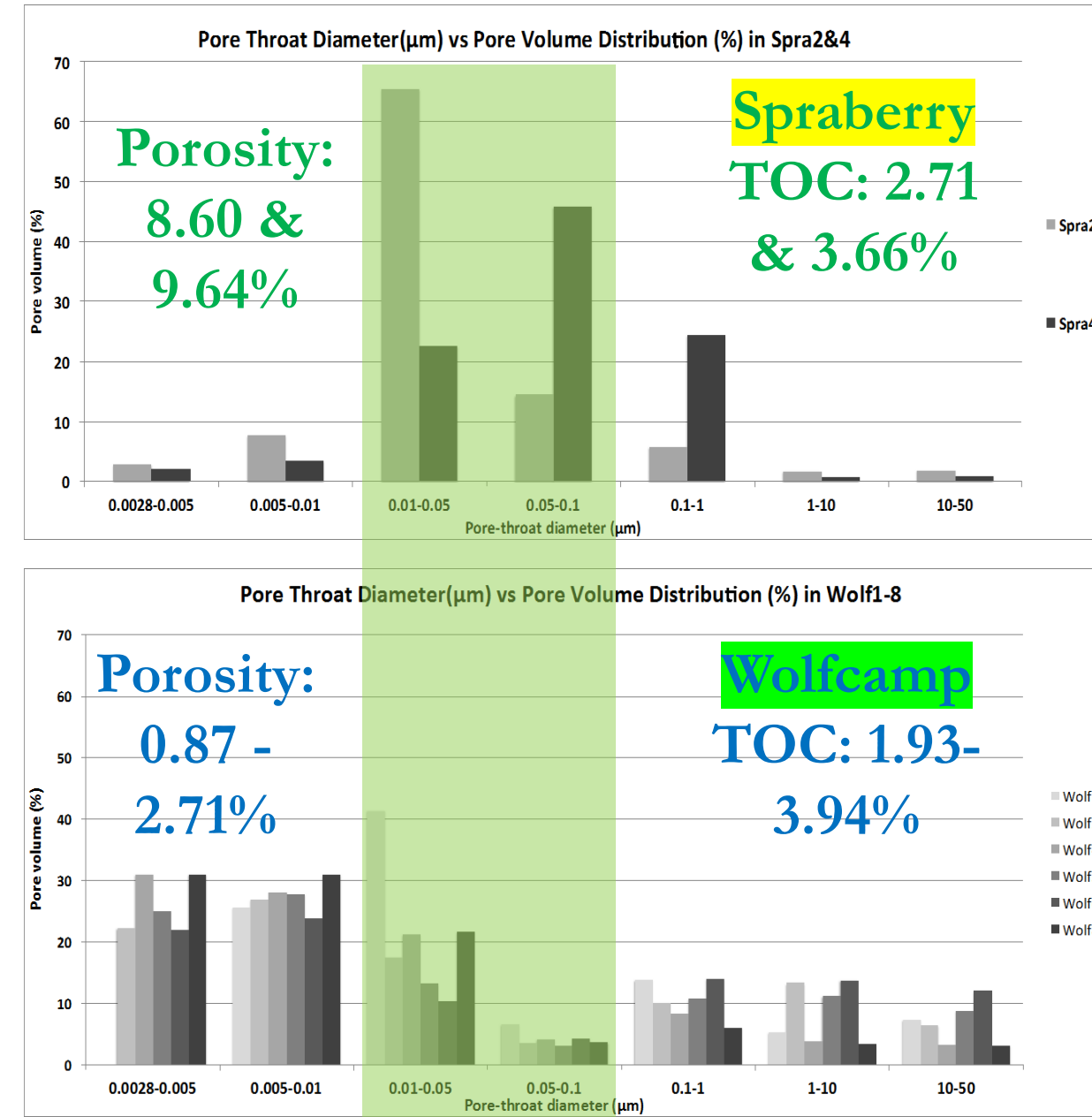
Midland Basin: Spraberry-Dean-Wolfcamp



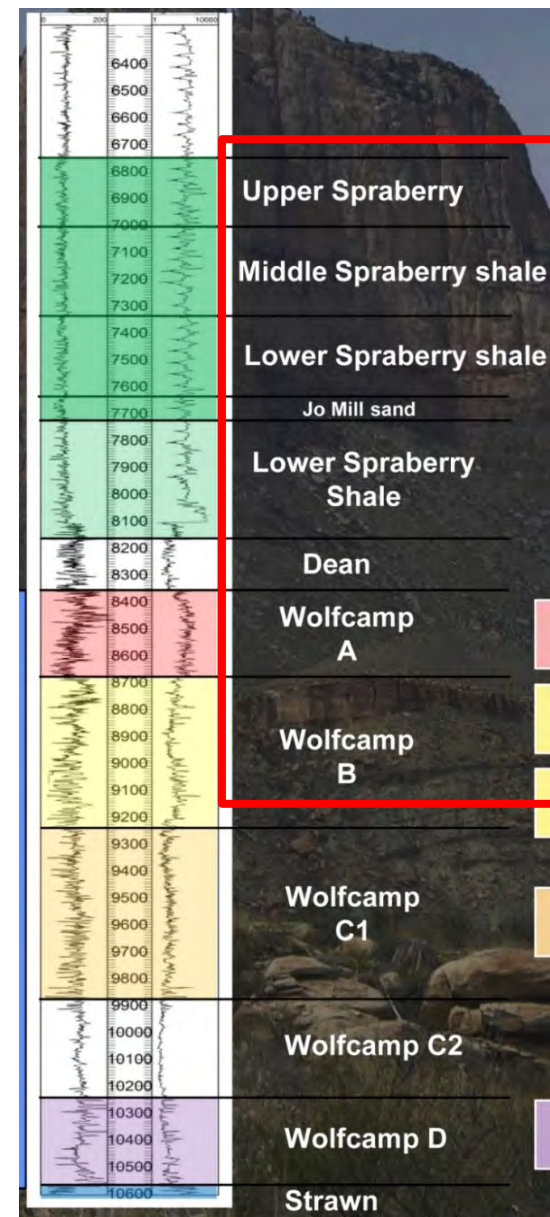
Ryan Quintero



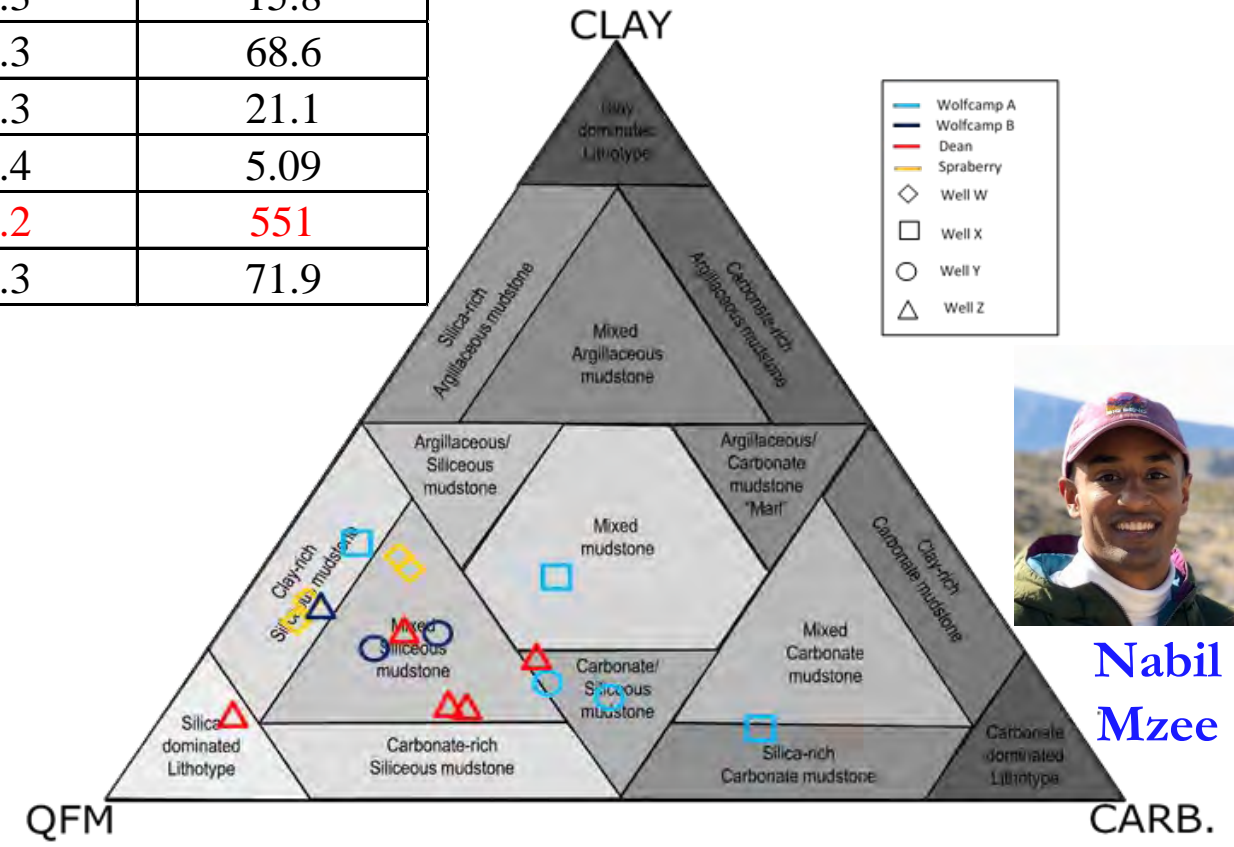
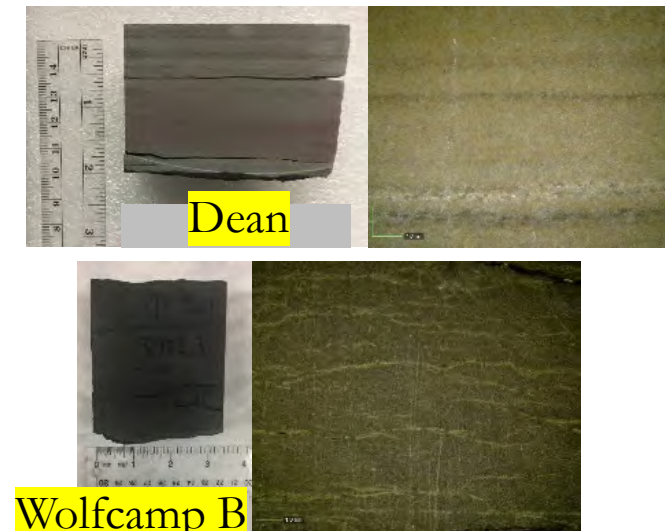
Hu et al., MPG, 2020



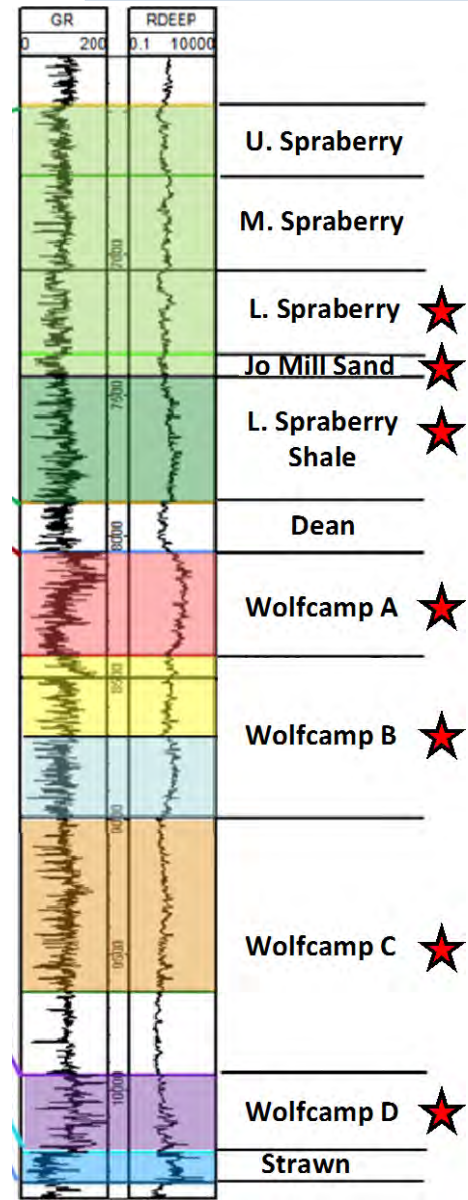
Midland Basin: Spraberry-Dean-Wolfcamp



	Pore-throat size (nm)	Pore-throat volume (%)	k (nD)
W537A SPRA	>100	58.0	321065
X340 WCa	2.8-50	59.3	1.21
X682 WCa	2.8-10	74.4	0.828
Y538 WCa	>100	55.4	486906
Y540 WCa	2.8-50	79.1	2.00
Y782 WCb	2.8-50	80.3	15.8
Y863 WCb	2.8-50	72.3	68.6
Z200 Dean	2.8-50	81.3	21.1
Z281 Dean	2.8-50	94.4	5.09
Z293 Dean	>100	85.2	551
Z823 WCb	2.8-50	58.3	71.9



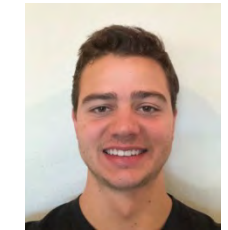
Midland Basin: Lower Spraberry-Wolfcamp A, B, C, D & Cisco and Canyon



Siliceous- Clay-rich Facies

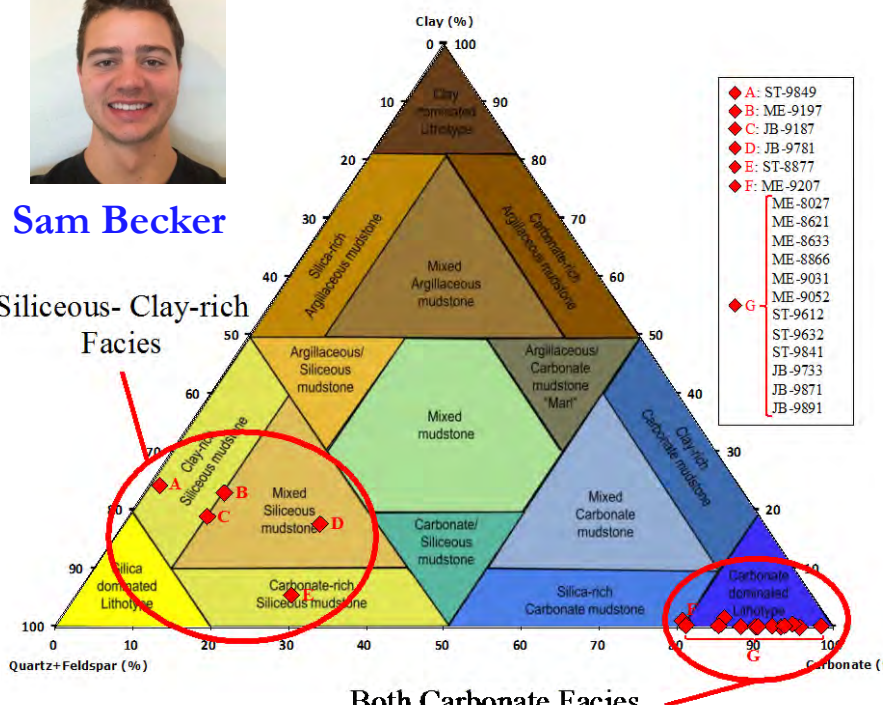


Porosity: 4.93 %
Permeability: 763 mD
TOC: 3.15 wt%
PI: 0.21

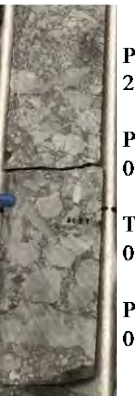


Sam Becker

Siliceous- Clay-rich Facies



Packestone and Grainstone



Porosity: 2.23 %
Permeability: 0.23 mD
TOC: 0.77 wt%
PI: 0.30

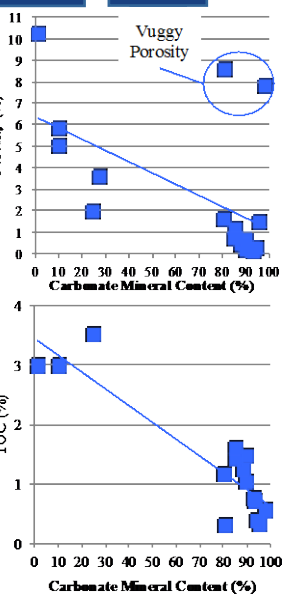
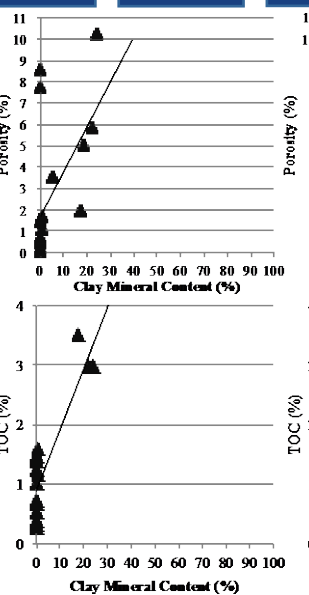
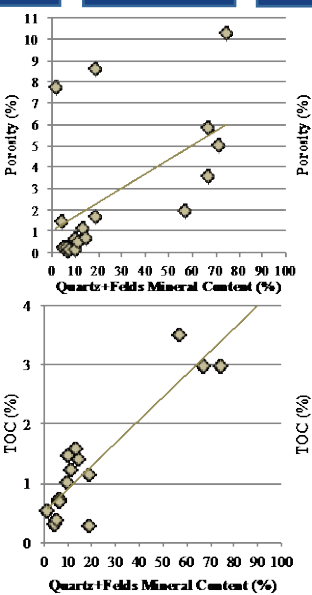


Porosity: 8.14 %

Carbonate Mudstone



Porosity: 1.75 %
Permeability: 0.37 mD
TOC: 1.08 wt%
PI: 0.24



Pore Space

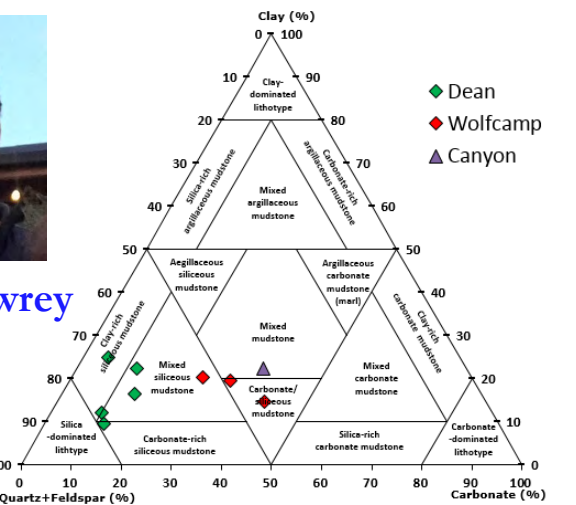
Sample ID	Pore Space					Geochemistry				
	MIP Porosity (%)	Permeability (mD)	Geometrical Tortuosity (L_e/L)	Imbibition Connectivity		Contact Angle	TOC (wt%)	S1 mg HC/g rock	S2 mg HC/g rock	Tmax (°C)
	DIW	DT2		Wettability						
ME-9197	5.85	6.68E-06	107.9	Low	High	Oil-Wet	2.99	1.49	4.41	437
ST-8877	3.51	7.50E-05	24.29	Low	Intermediate	Water-Wet	-	-	-	-
ST-9849	10.20	3813	0.21	Low	High	Oil-Wet	2.97	2.21	5.84	437
JB-9187	5.02	6.19E-05	30.19	Low	High	-	-	-	-	-
JB-9781	1.95	1.83E-06	8.74	High	Low	Intermediate	3.50	1.65	13.45	436
ME-8027	0.11	0.07	0.09	Low	High	Partial Oil-Wet	-	-	-	-
ME-8621	0.44	4.96E-07	3.81	Low	Low	Oil-Wet	1.23	0.73	2.14	440
ME-8633	1.47	7.29E-05	2.21	Low	Intermediate	Intermediate	0.32	0.18	0.36	438
ME-9052	8.53	1.18	3.46	Low	Intermediate	Oil-Wet	0.29	0.35	0.53	436
ME-9207 (FIP)	-	-	-	Low	Low	Oil-Wet	1.16	0.82	1.53	437
ST-9612	0.63	1.02E-06	3.85	High	High	Oil-Wet	1.02	0.86	1.90	432
ST-9841	7.75	0.52	4.36	Intermediate	High	Oil-Wet	0.54	1.08	1.46	427
JB-9733	1.09	1.90E-06	5.64	Low	High	Intermediate	1.58	0.97	5.45	436
JB-9871	0.16	0.04	0.15	Low	-	Oil-Wet	0.38	0.22	0.93	429
ME-8621	0.70	0.71	0.23	Low	Low	Partial Oil-Wet	1.40	0.72	2.35	440
ME-8866	0.04	0.31	0.04	Low	High	Oil-Wet	0.74	0.43	0.97	437
ST-9632	0.15	0.19	0.08	Low	High	Intermediate	1.47	1.34	2.75	443
JB-9891	0.17	0.28	0.1	Low	High	Intermediate	0.69	0.16	1.32	435

Midland Basin: Dean-Wolfcamp

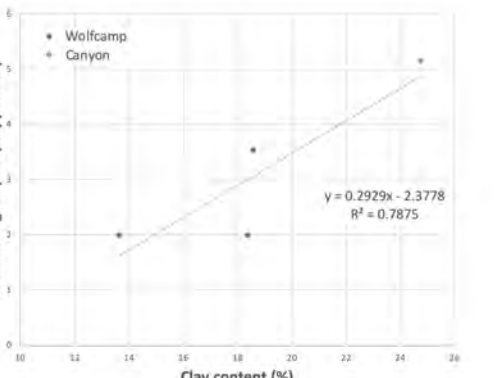
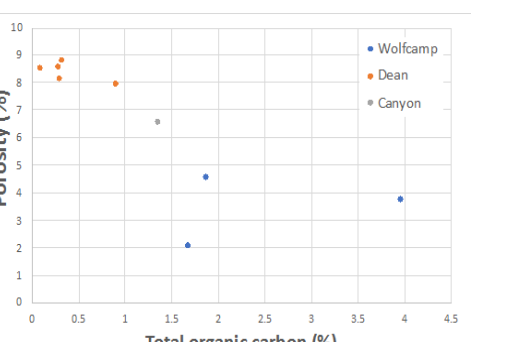
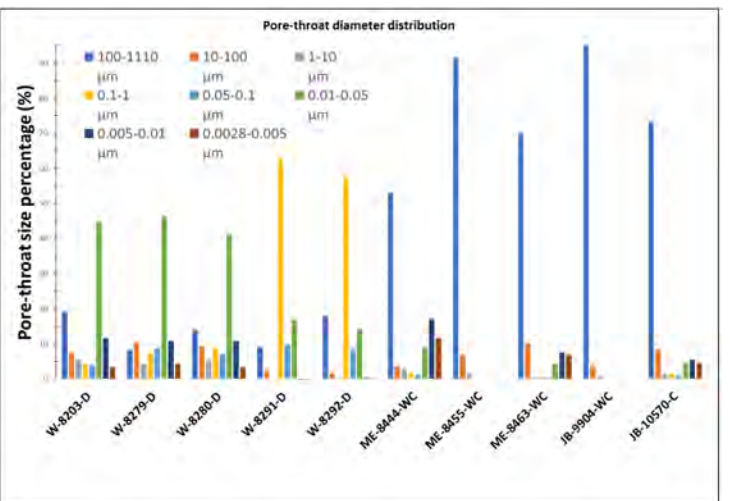
System	Series	Midland Basin Formations
Permian	Ochoan	Dewey Lake
		Rustler
		Salado
	Guadalupian	Tansill
		Yates
		Seven Rivers
		Queen
		Grayburg
	Leonardian	San Andres
		San Angelo
		Upper Leonard
		Spraberry
		Dean
Pennsylvanian	Wolfcampian	Wellcamp A
		Wellcamp B
		Wellcamp C
		Wellcamp D
	Clearfork	Clearfork
		Canyon
		Wolfcamp
Mississippian	Canyon	Wolfcamp D
		Wolfcamp
	Strawn	Strawn
		Lime
		Sharktooth
Atokan	Atoka	Atoka
		Sand Lst
		Sh. & Sh. Sand
Morrowan	Morrow	Morrow



Benton Mowrey



Sample ID	Contact Angle (°)			
	DIW	API Brine	THF	n-decane
W-8203-D	24.1	23.3	14.6	9.0 - 1.5
W-8279-D	1.5-4.4	8.9	6.4	11.7 - 1.5
W-8280-D	1.5	18.4	1.9	10.1 - 1.5
W-8291-D	32.6	45.9	23.1	10.1 - 1.5
W-8292-D	22.7	39.3	12.0	15.1 - 1.5
ME-8444-WC	39.1	51.2	20.0	65.2 - 58.3



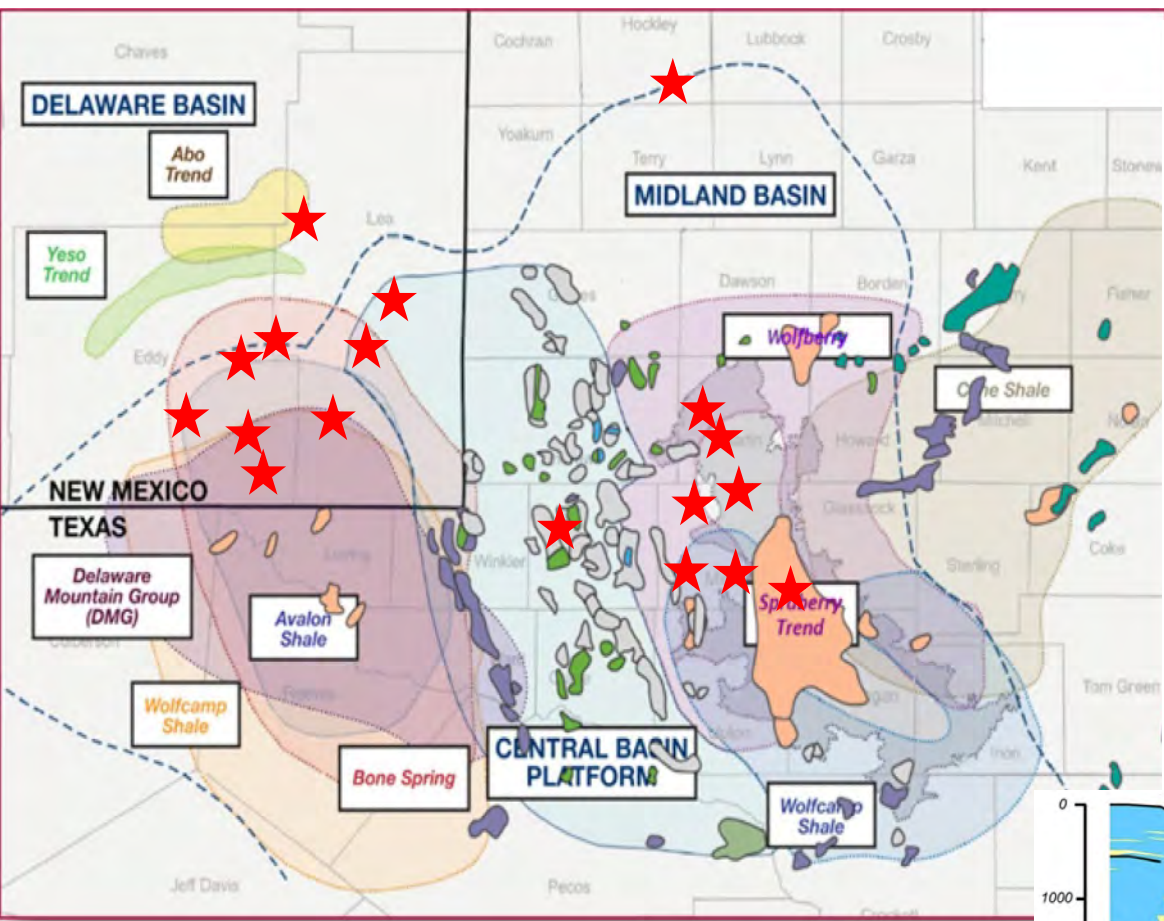
Sample ID	Predominant (>100 nm) pore-throat network		Predominant (2.8-50 nm) pore-throat network		Gao and Hu Permeability k_{GH} (mD)
	Permeability k_{100} (mD)	Effective tortuosity	Permeability $k_{2.8-50}$ (mD)	Effective tortuosity	
W-8203-D	3.17E+02	18.9	5.93E-05	39742	5.72E-05
W-8279-D	1.92E+01	45.6	7.41E-05	23181	1.22E-04
W-8280-D	1.99E+01	48.1	5.62E-05	28590	1.04E-04
W-8291-D	6.74E-02	789.2	7.35E-04	7561	7.13E-03
W-8292-D	4.82E-01	483.4	1.14E-04	29981	7.26E-03
ME-8444-WC	8.61E+03	4.3	8.24E-06	138798	4.26E+04
ME-8455-WC	1.12E+04	3.2	-	-	1.85E+05
ME-8463-WC	4.79E+03	4.7	1.10E-05	116605	4.19E+04
JB-9904-WC	2.07E+04	2.5	-	-	3.38E+05
JB-10570-C	1.51E+04	4.3	1.33E-05	145123	8.33E+04

Sample ID	Bulk density (g/cm³)	Skeletal density (g/cm³)	Porosity (%) (g/cm³)
	Sample ID	Connectivity Slope	
W-8203-D	2.393	2.599	7.95
W-8279-D	2.435	2.650	8.12
W-8280-D	2.422	2.648	8.55
W-8291-D	2.426	2.651	8.51
W-8292-D	2.435	2.669	8.78
ME-8444-WC	2.461	2.556	3.73
ME-8455-WC	3.049	3.113	2.05
ME-8463-WC	2.345	2.457	4.56
JB-9904-WC	2.536	2.580	1.69
JB-10570-C	2.416	2.595	6.54

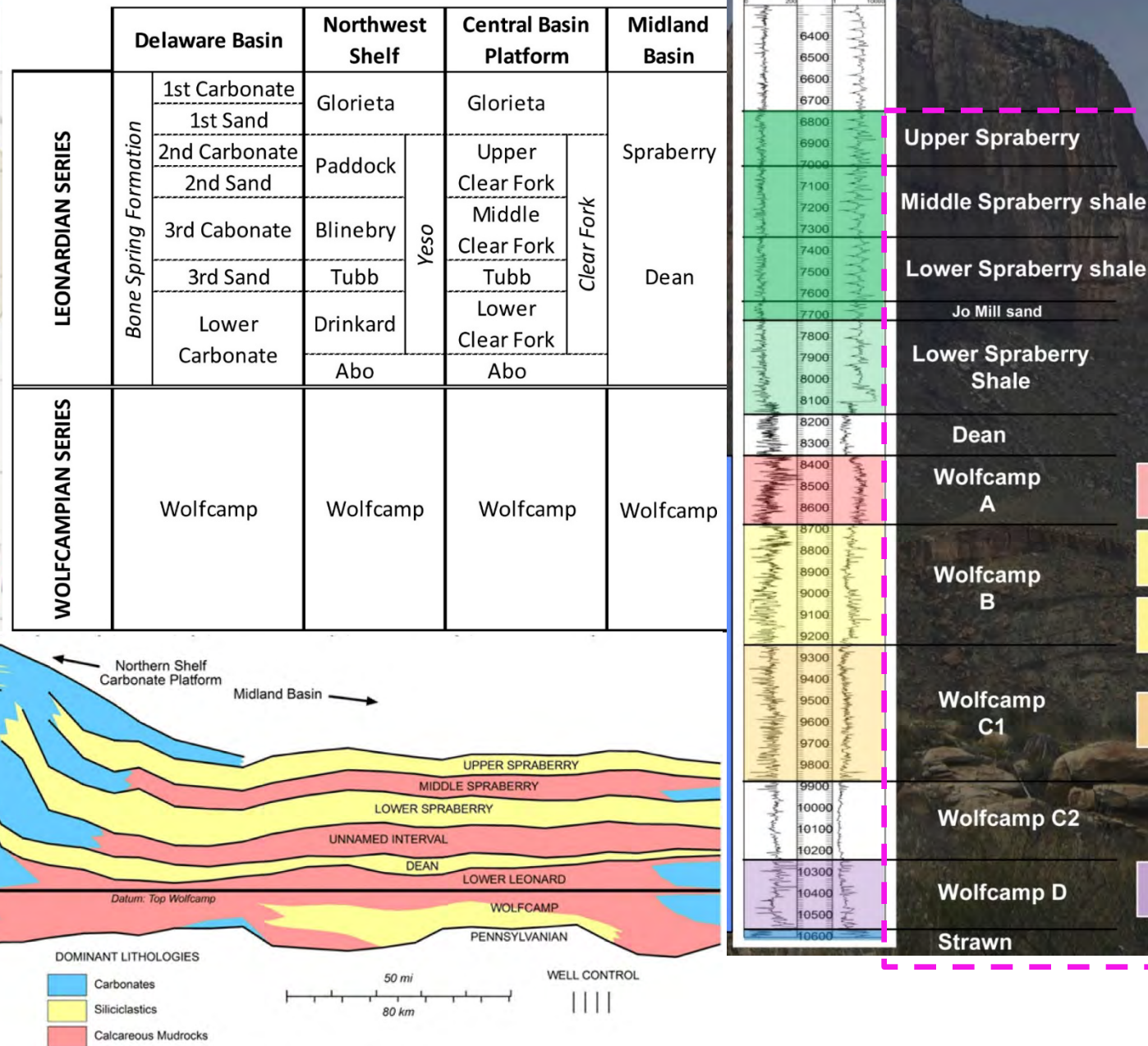
Sample ID	DIW	DT2
W-8203-D	0.277	0.581
W-8279-D	0.312	0.895
W-8280-D	0.514	0.368
W-8291-D	0.198	0.586
W-8292-D	0.193	0.621
ME-8444-WC	0.308	0.673
ME-8455-WC	0.130	0.602
ME-8463-WC	0.233	0.575
JB-9904-WC	0.267	0.249
JB-10570-C	0.188	1.961

Sample ID	Slab (~4 cm across)			Cubes (1 cm³)		
	DI Water			DT2		
Sample ID	Porosity (%)	Bulk Density (g/cc)	Grain Density (g/cc)	Porosity (%)	Bulk Density (g/cc)	Grain Density (g/cc)
W-8203-D	7.439	2.341	2.530	7.538 ± 0.120	2.428 ± 0.007	2.626 ± 0.010
W-8279-D	8.004	2.466	2.681	11.209 ± 1.244	2.427 ± 0.008	2.734 ± 0.043
W-8280-D	9.021	2.339	2.571	9.646 ± 0.017	2.391 ± 0.015	2.646 ± 0.017
W-8291-D	7.146	2.461	2.651	10.399 ± 2.54	2.437 ± 0.021	2.722 ± 0.088
W-8292-D	6.25	2.462	2.626	9.600 ± 2.609	2.443 ± 0.054	2.704 ± 0.111
ME-8444-WC				0.895 ± 0.198	2.462 ± 0.020	2.485 ± 0.015
ME-8455-WC				0.846 ± 0.443	2.595 ± 0.002	2.617 ± 0.014
ME-8463-WC				1.485 ± 0.646	2.531 ± 0.014	2.569 ± 0.021
JB-9904-WC				3.027 ± 2.997	2.582 ± 0.007	2.671 ± 0.085
JB-10570-C				3.667 ± 0.138	2.561 ± 0.019	2.621 ± 0.023

Permian Basin

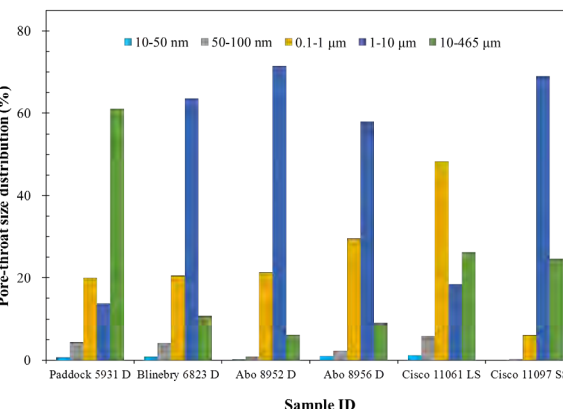


- 86,000 sq. miles (2.26% USA)
- 52 counties



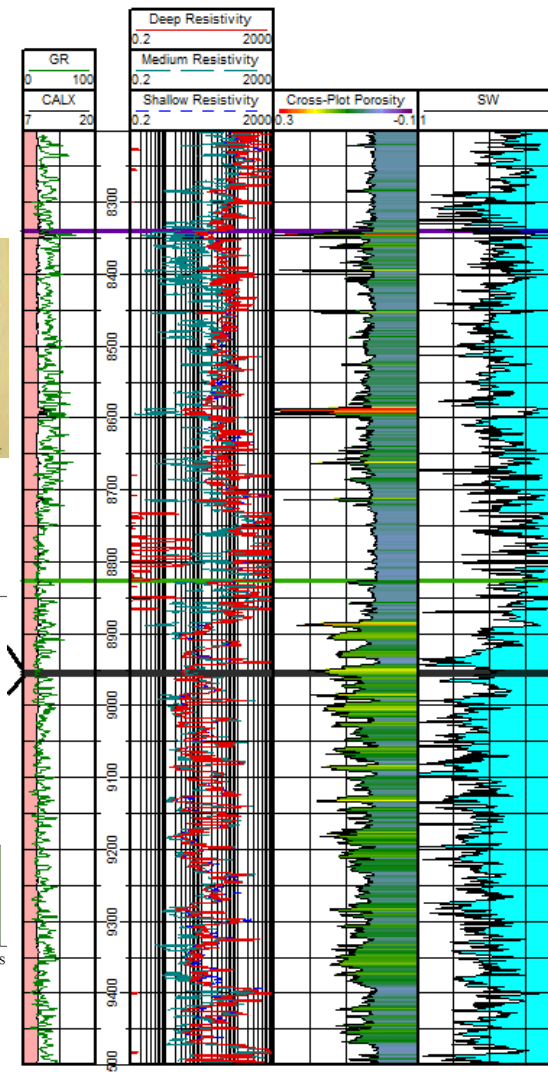
Northwest Shelf: Carbonates

System	Northwest Shelf	
Permian	Dewey Lake	
	Rustler	
	Salado	
	Tansill	
	Whiteln Horse	
	Yates	
	7 Rivers	
	Queen	
	Grayburg	
	Word	Goat Seep - Capitan Reef
	San Andres	
	Glorietta	
	Paddock	
	Blueberry	
	Tubb	
	L. Clearfork	
	Abo	
	Wolfcamp	
	Cisco	
	Canyon	
	Strawn	
	Atoka	
	Morrow	



Majority of pore throats fall in the range of 1-10 μm

ConocoPhillips
Gen Montcalm 25 State #1



Abo 8952 D

Griffin Mann

Porosity (%)	Permeability (mD)
Cross-plot (Log)	17.9
Boyle's Law porosimeter	20.9
MICP	17.9

Abo 8956 D

Porosity (%)	Permeability (mD)
Cross-plot (Log)	14.8
Boyle's Law porosimeter	14.7
MICP	15.9

Permeability (mD)

Log-derived	2.8
Hassler Sleeve permeameter	0.91



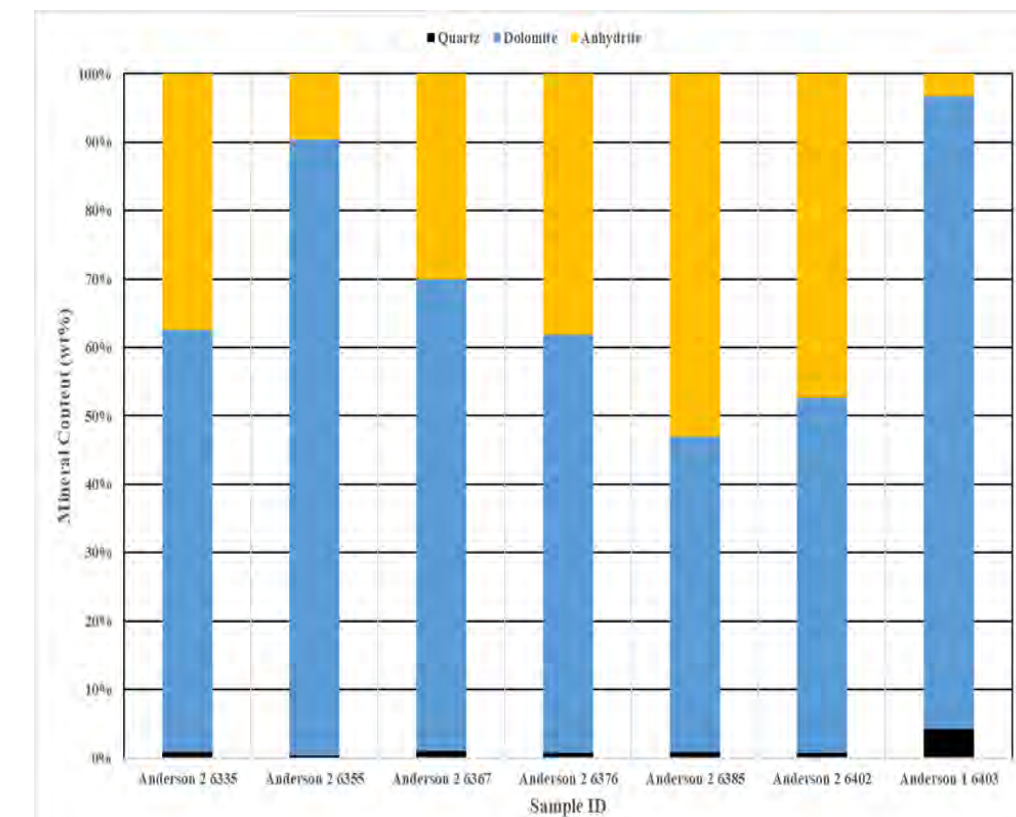
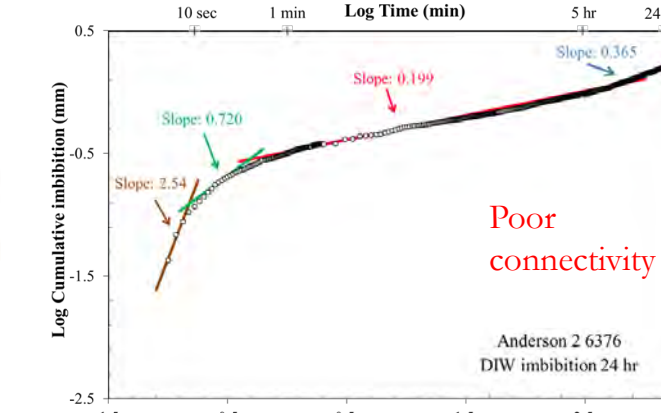
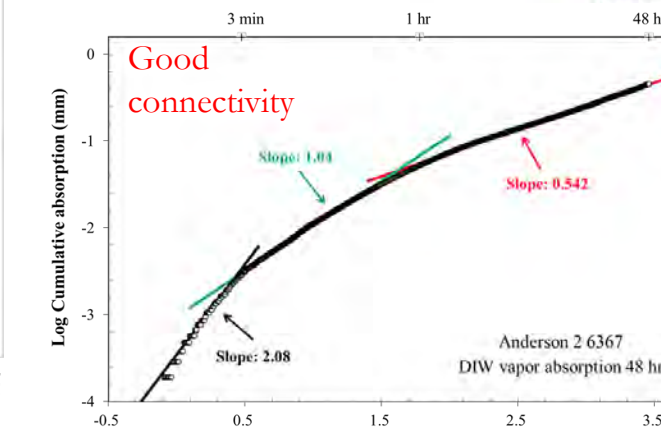
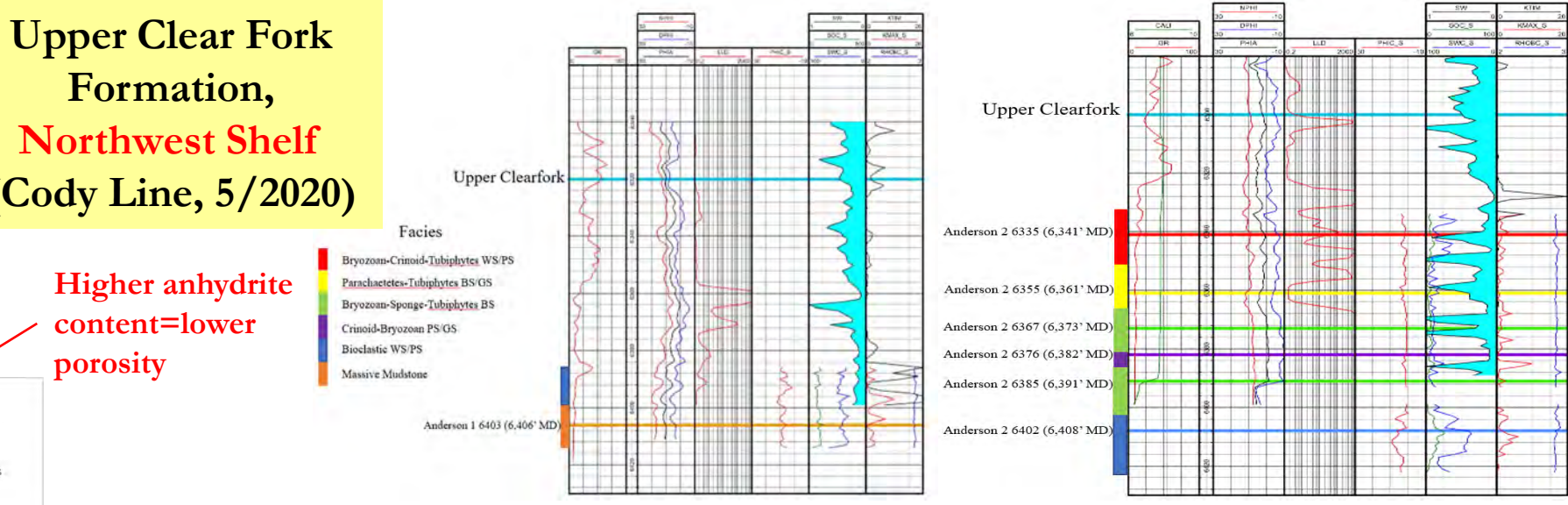
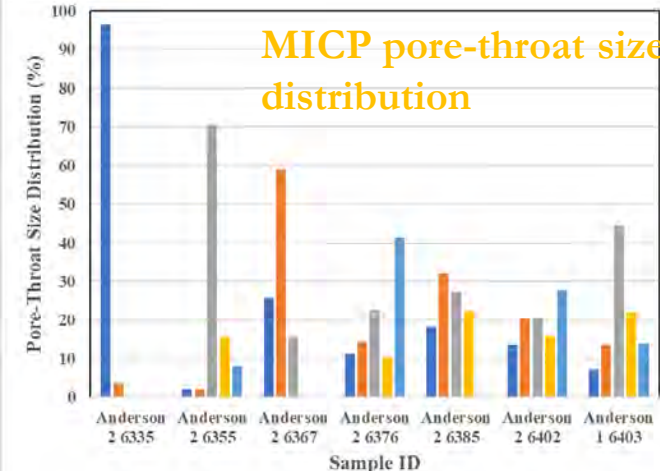
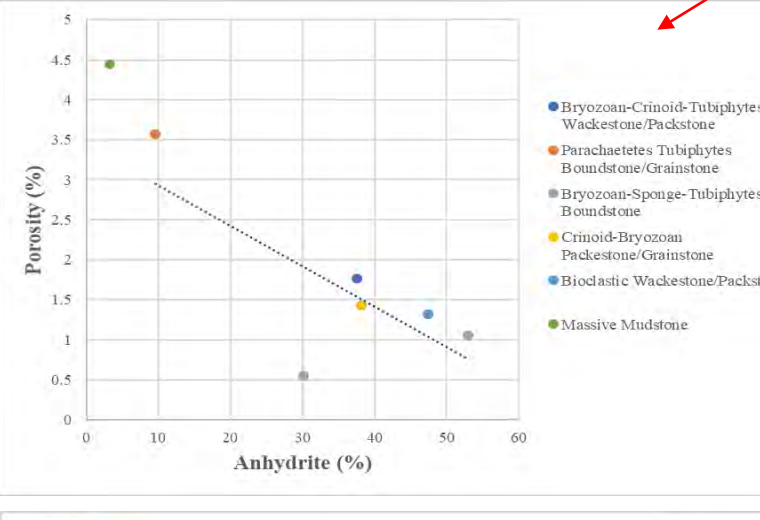
SUBSURFACE		
CENTRAL BASIN PLATFORM NEW MEXICO		NORTHERN SHELF TEXAS
SERIES	STAGE	
Lower Permian	LEONARDIAN	San Andres
	Glorieta	Glorieta
Yoso	Paddock	upper Clear Fork
	Blinebry	middle Clear Fork
	Tubb	Tubb
	Drinkard	lower Clear Fork
	Abo	Wichita Group
	Wolfcamp	Wolfcamp



Cody Line

Upper Clear Fork Formation, Northwest Shelf (Cody Line, 5/2020)

Higher anhydrite content=lower porosity



Median Pore-throat: Shale Gas (<2.8-20 nm) vs. Tight Oil (5-50 nm)

Molecular sizes

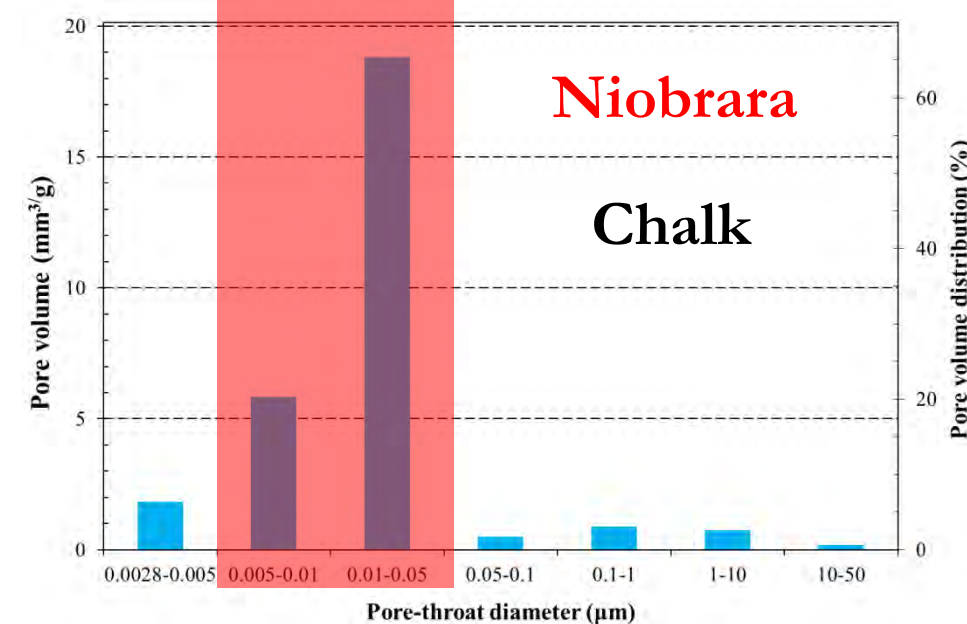
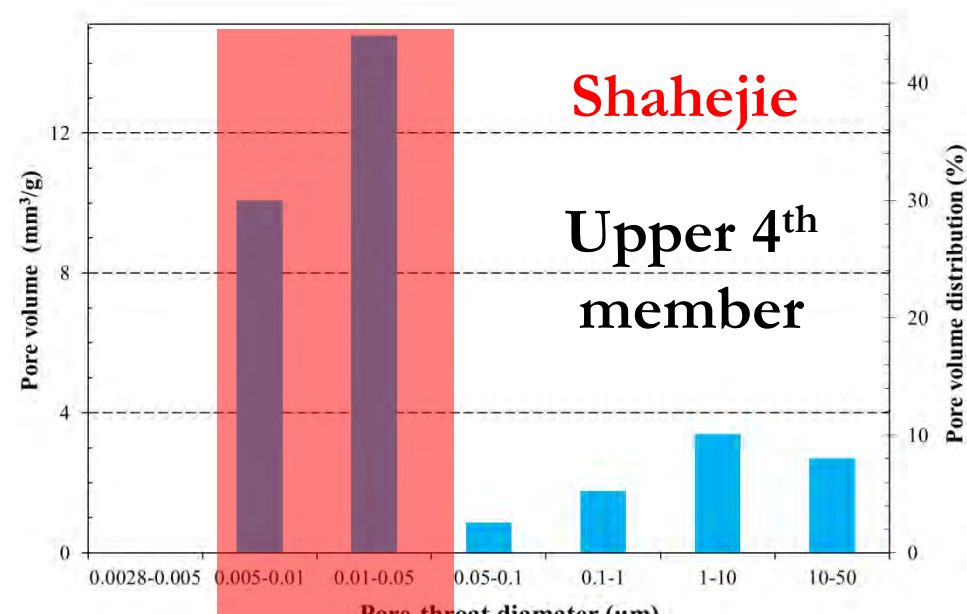
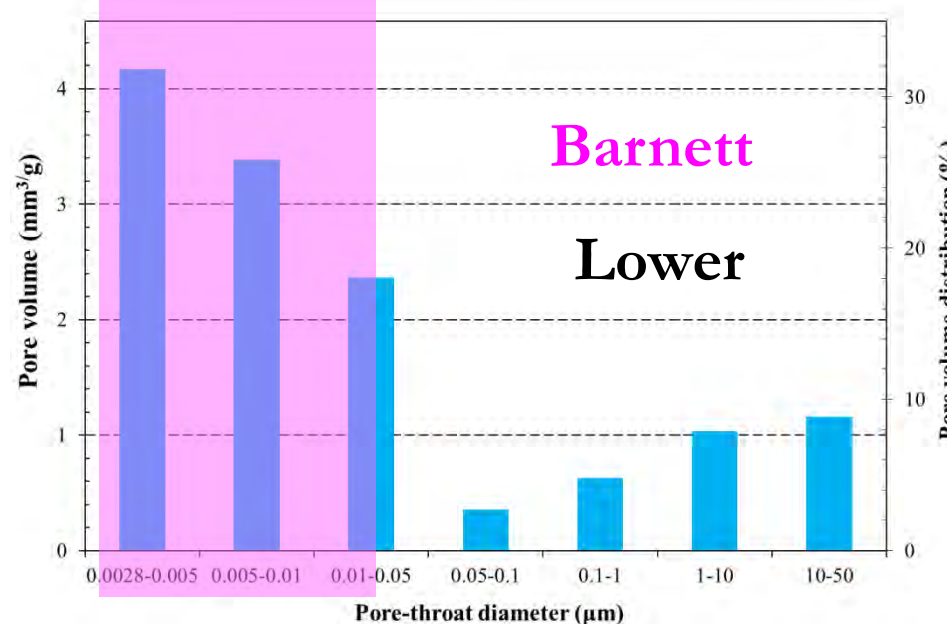
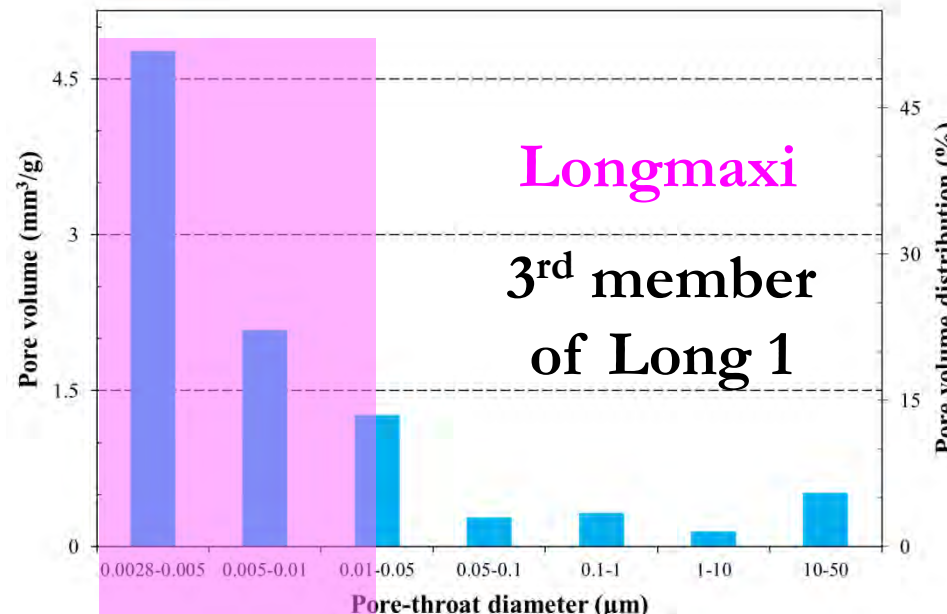
H_2O : 0.32 nm

CH_4 : 0.38 nm

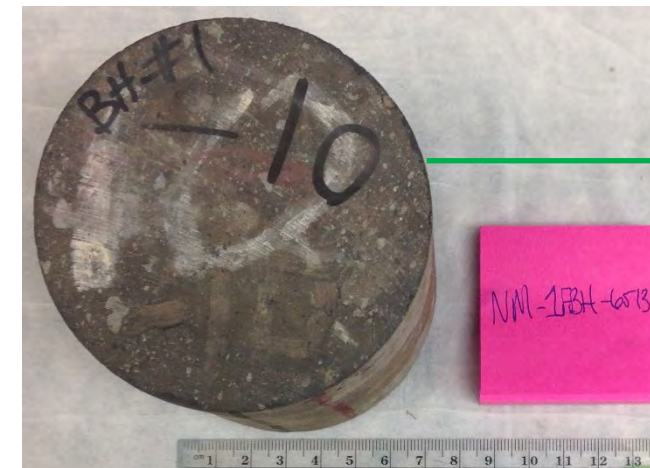
Aromatics: 1-3 nm

Paraffin: 5-10 nm

(Nelson, 2009)

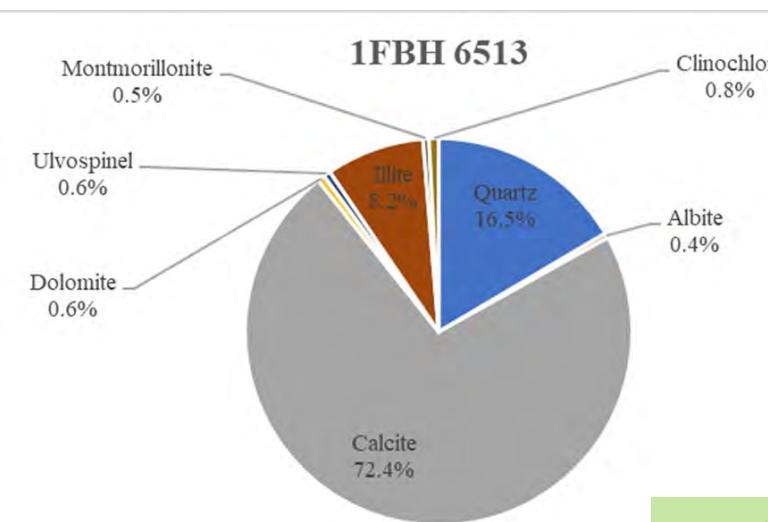


Pore Connectivity-related Size-Dependent Effective Porosity: Wolfcamp A Shale

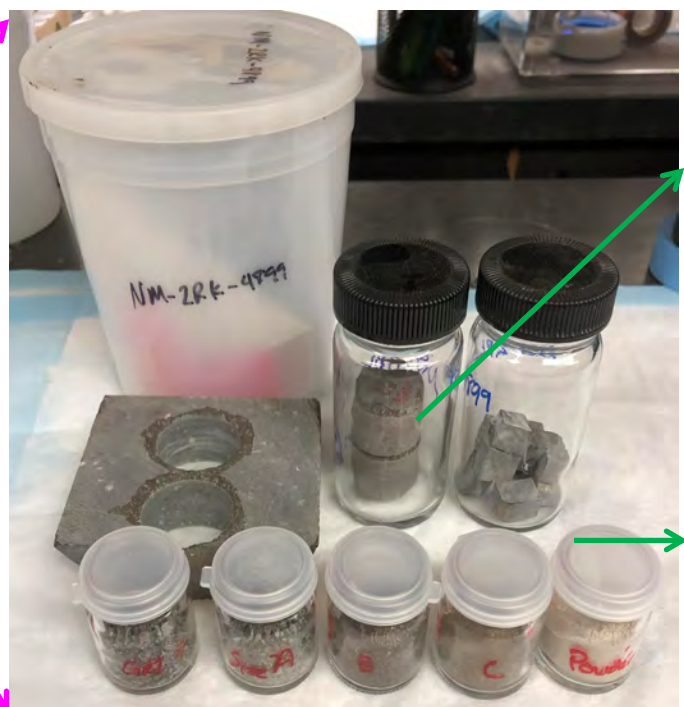
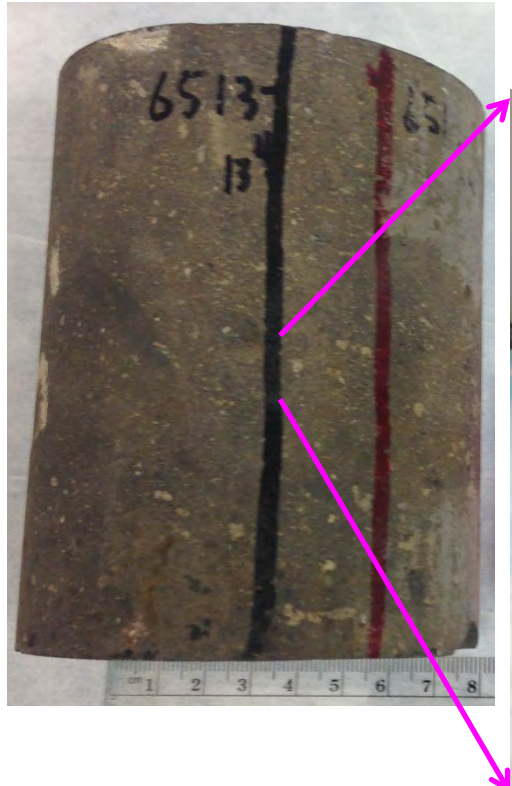


Vacuum saturation DI Water

- ✓ D_e : 10.49 cm
- ✓ φ : 1.134%
- ✓ ρ_b : 2.635 g/cm³
- ✓ ρ_p : 2.666 g/cm³



Silica-rich
carbonate
mudstone



- ✓ D_e : 3.008 ± 0.199 cm
- ✓ φ : 2.107 ± 0.327 %
- ✓ ρ_b : 2.639 ± 0.027 g/cm³
- ✓ ρ_p : 2.695 ± 0.018 g/cm³

- ✓ D_e : 1.438 ± 0.011 cm
- ✓ φ : 2.531 ± 0.358 %
- ✓ ρ_b : 2.608 ± 0.024 g/cm³
- ✓ ρ_p : 2.676 ± 0.015 g/cm³

2 DT (n-decane : toluene)

- ✓ φ : 3.185%
- ✓ ρ_b : 2.638 g/cm³
- ✓ ρ_p : 2.725 g/cm³

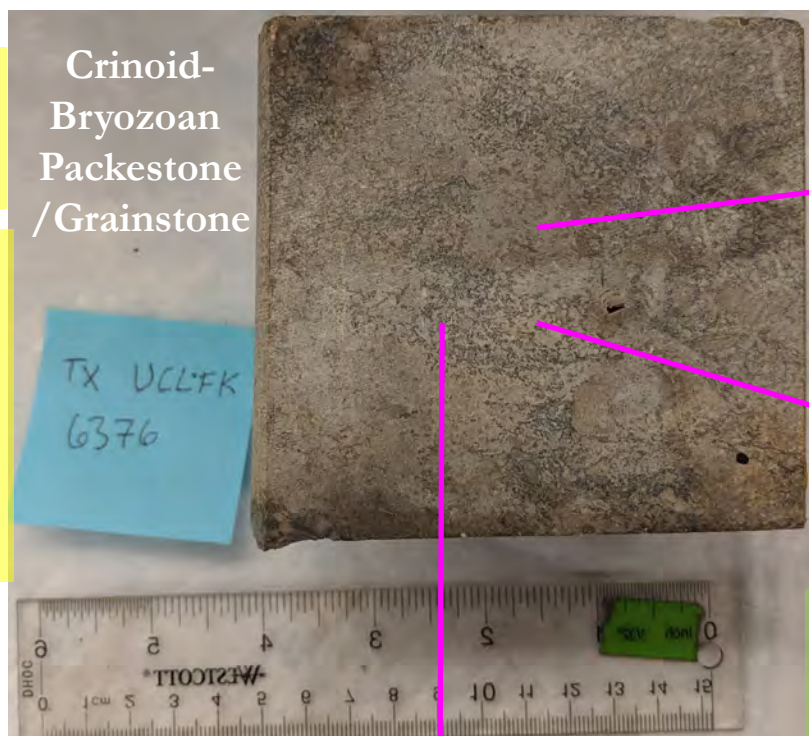
THF (tetrahydrofuran)

- ✓ φ : 2.500%
- ✓ ρ_b : 2.576 g/cm³
- ✓ ρ_p : 2.642 g/cm³

Pore Connectivity-related Size-Dependent Effective Porosity: Upper Clear Fork Carbonate

Vacuum saturation
DI Water

- ✓ $D_e: 10.15 \text{ cm}$
- ✓ $\varphi: 0.347\%$
- ✓ $\rho_b: 2.716 \text{ g/cm}^3$
- ✓ $\rho_p: 2.7263 \text{ g/cm}^3$



MIP

- ✓ $\varphi: 1.30\%$
- ✓ $\rho_b: 2.812 \text{ g/cm}^3$
- ✓ $\rho_p: 2.850 \text{ g/cm}^3$

- ✓ $D_e: 3.29 \pm 0.069 \text{ cm}$
- ✓ $\varphi: 0.983 \pm 0.347\%$
- ✓ $\rho_b: 2.686 \pm 0.046 \text{ g/cm}^3$
- ✓ $\rho_p: 2.735 \pm 0.064 \text{ g/cm}^3$

- ✓ $D_e: 1.27 \pm 0.012 \text{ cm}$
- ✓ $\varphi: 1.431 \pm 0.319\%$
- ✓ $\rho_b: 2.613 \pm 0.161 \text{ g/cm}^3$
- ✓ $\rho_p: 2.651 \pm 0.182 \text{ g/cm}^3$

Well log ✓ $\varphi: -1.30\%$

✓ $D_e: 0.203 \text{ cm}$
✓ $\rho_p: 2.8572 \pm 0.0007 \text{ g/cm}^3$

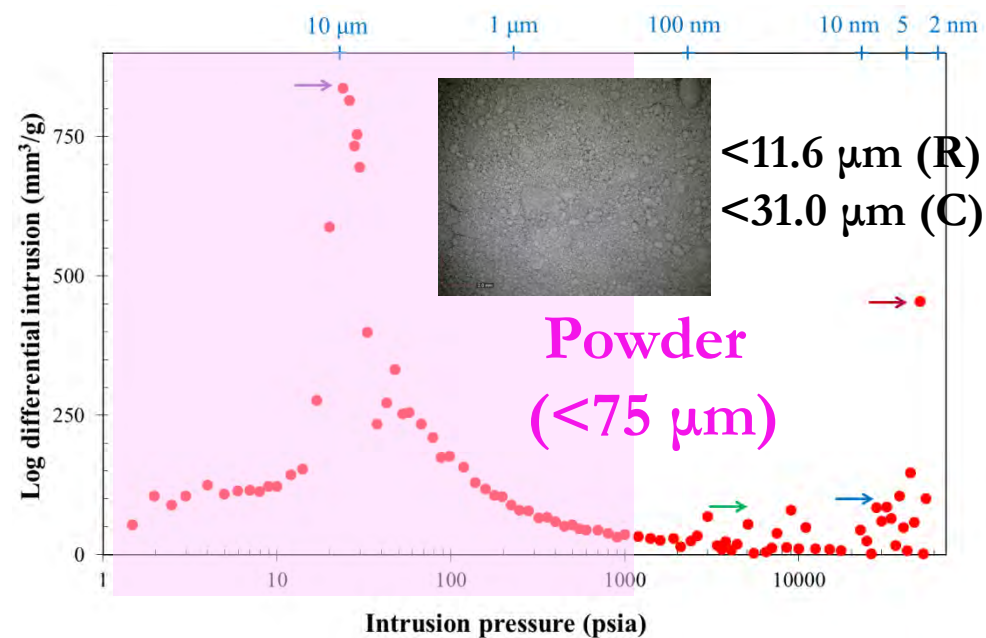
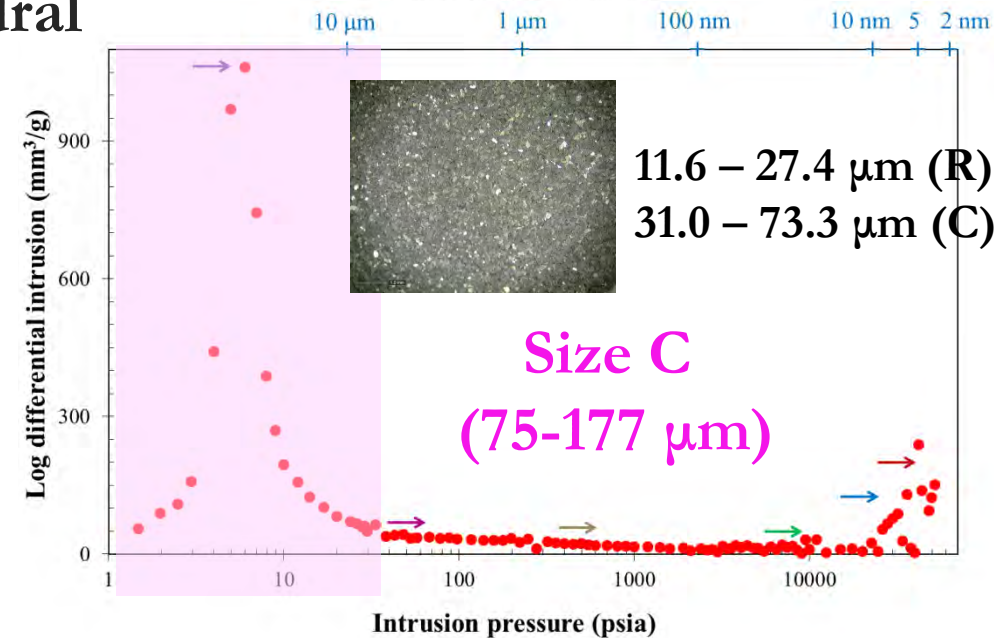
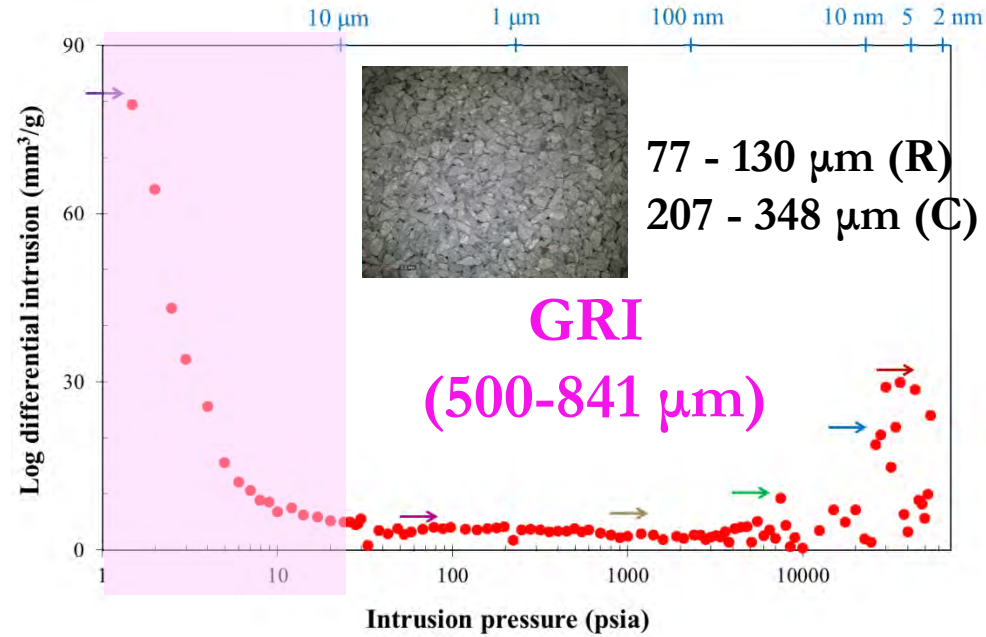
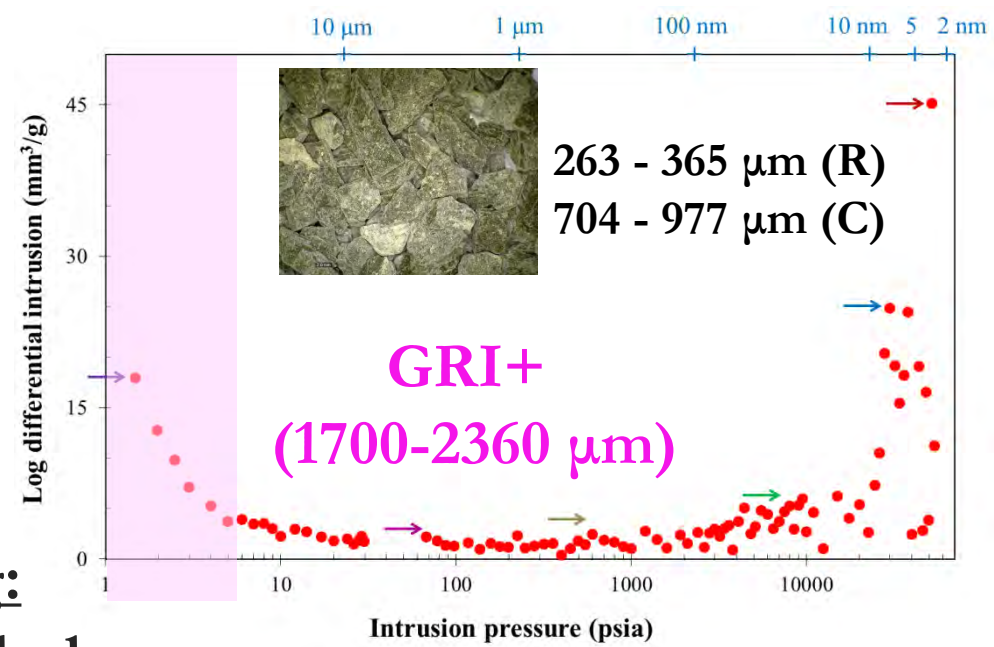
✓ $D_e: 0.127 \text{ cm}$
✓ $\rho_p: 2.8575 \pm 0.0040 \text{ g/cm}^3$



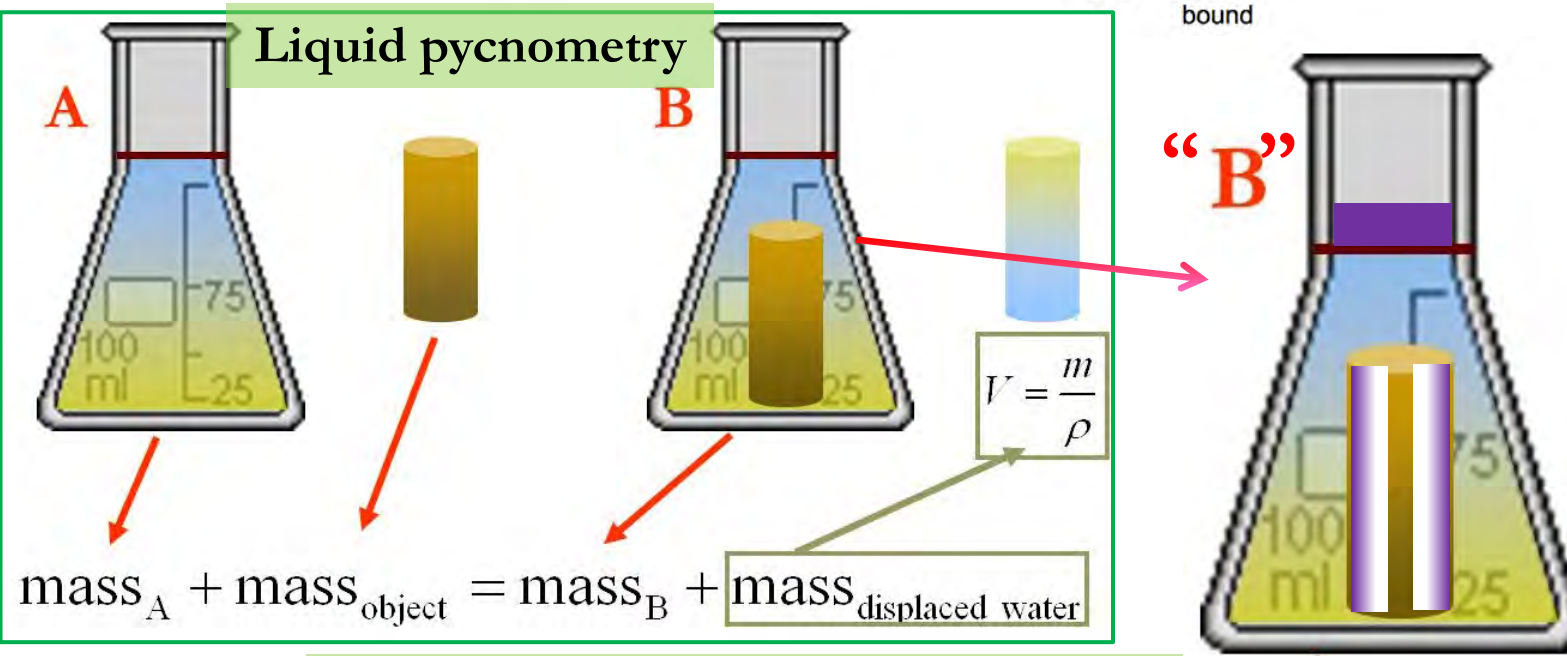
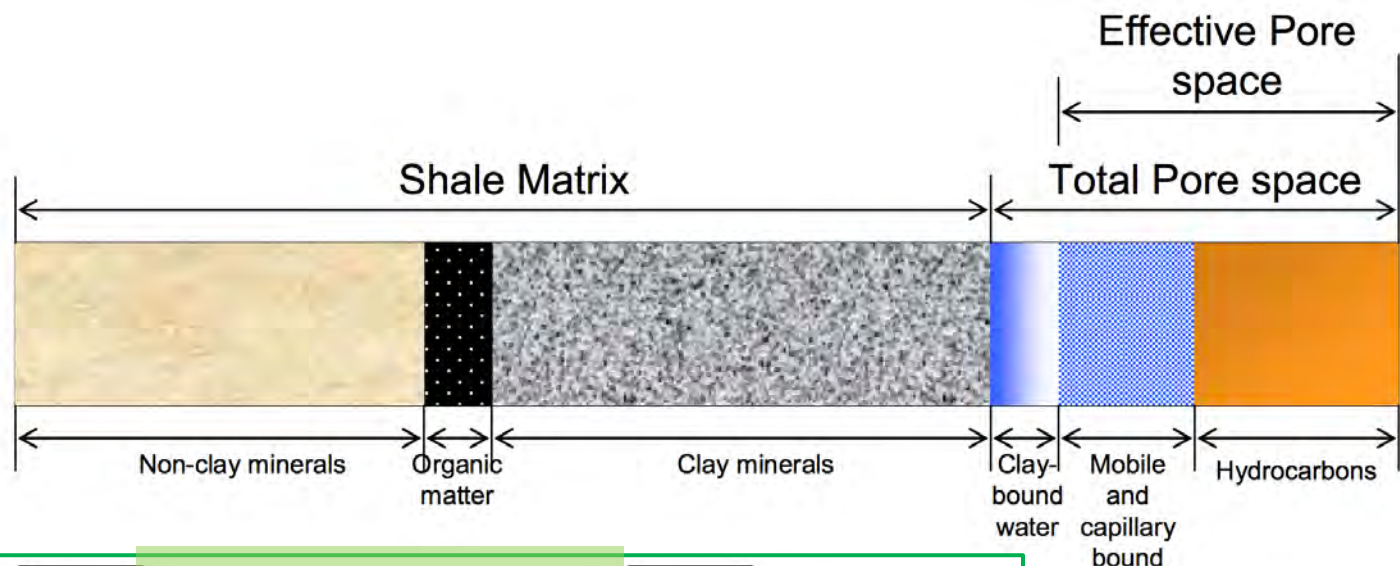
$$n = 1 - \frac{\rho_b}{\rho_p}$$

Wolfcamp Sample of Different Sizes: Inter- vs. Intra-granular Pores

Packing:
Rhombohedral
(R)
Cubic (C)



Total ϕ_t vs. Effective Porosity ϕ_e



originally designed for **SOLID** samples

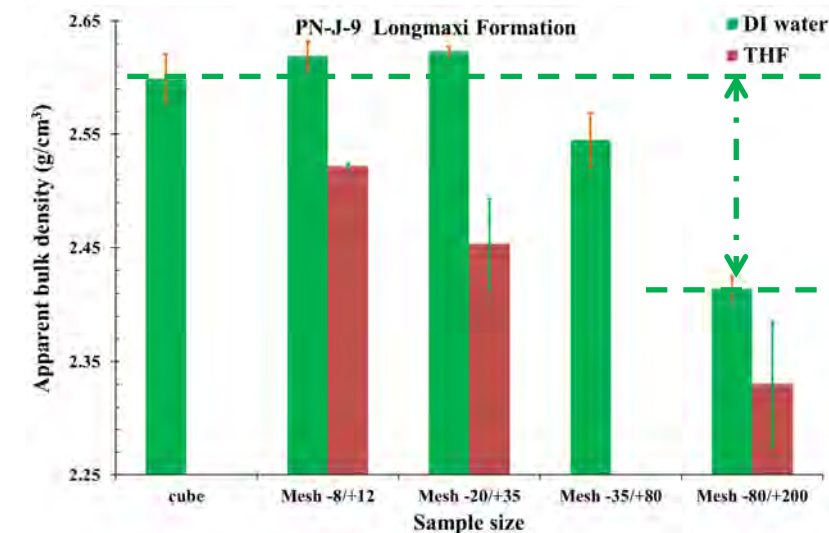
water-wet pores%

oil-wet pores%

and their distributions?

Apparent “bulk” density (fluid saturation) for relative comparison to assess sample size-dependent effective porosity towards a fluid

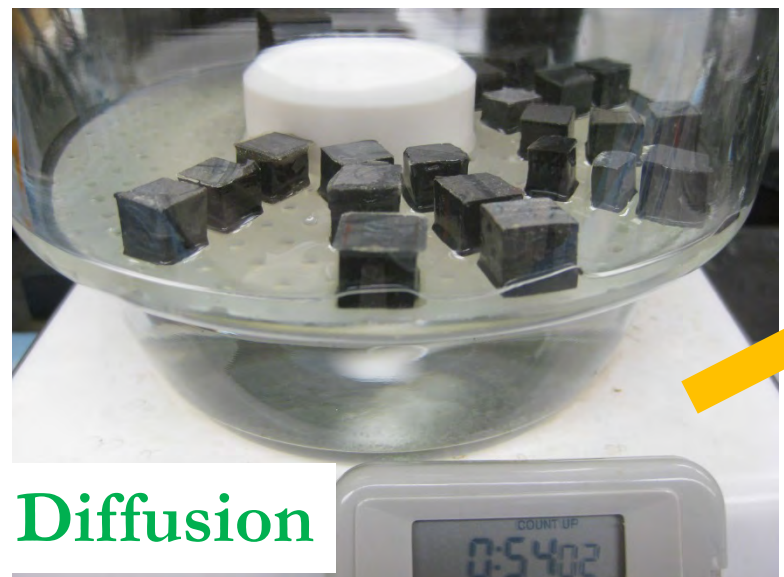
An increase of 7% in “porosity”



Different Tracer Tests for Process-Level Understanding

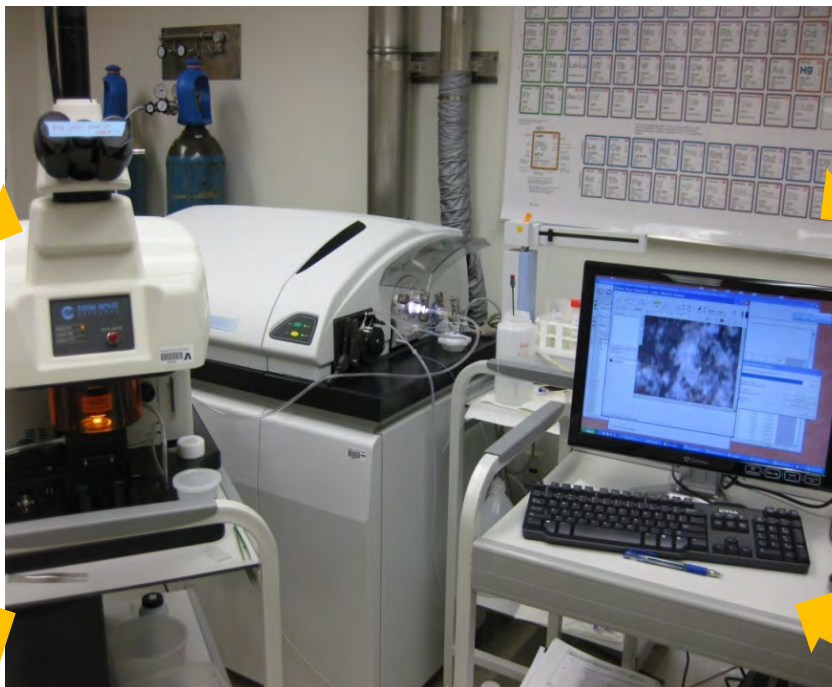


Imbibition



Diffusion

Laser Ablation-Inductively
Coupled Plasma-Mass
Spectrometry (LA-ICP-MS)



Hu et al., VZJ, 2004; GJ, 2012



Vacuum saturation

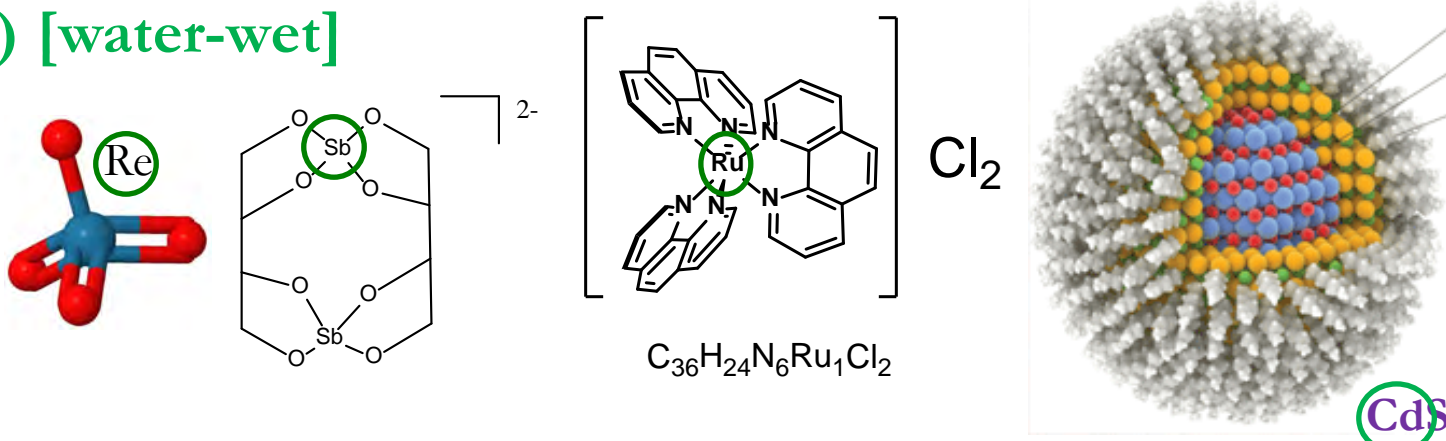


High-pressure impregnation

Wettability-based Fluids and Tracers

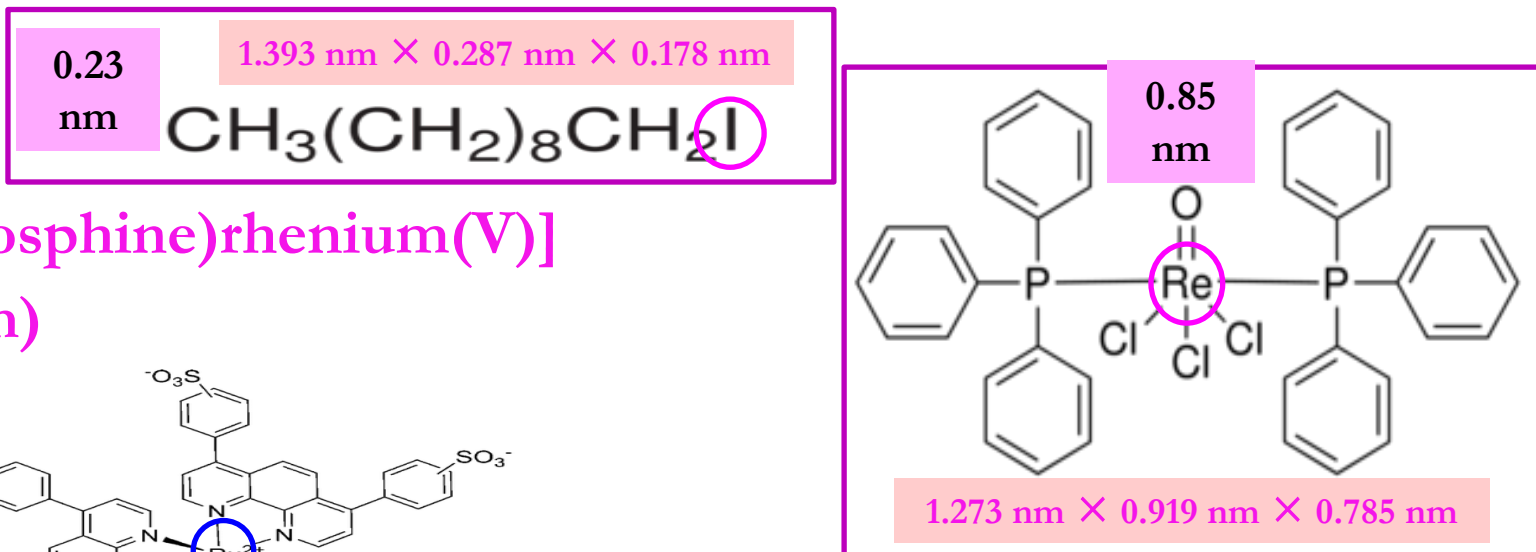
- API brine (8 wt% NaCl+2 wt% CaCl₂) [water-wet]

- ✓ ReO₄⁻ (0.553 nm)
- ✓ Anionic Sb-complex (0.89 nm)
- ✓ Cationic Ru-complex (1.0 nm)
- ✓ CdS nanoparticles (5–10 nm)



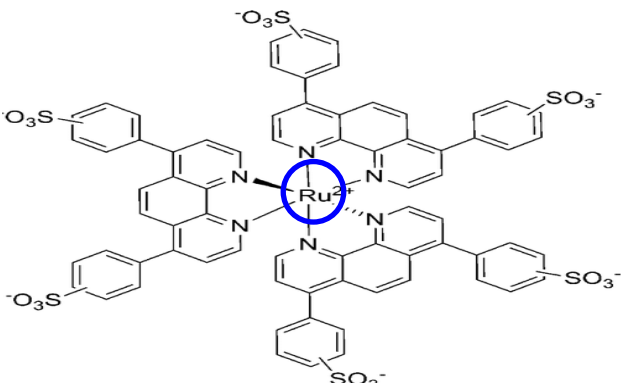
- n-decane: toluene [oil-wet]

- ✓ Organic-I (1-iododecane)
- ✓ Organic-Re
[trichlorooxobis(triphenylphosphine)rhenium(V)]
- ✓ CeF₃ nanoparticles (10–12 nm)



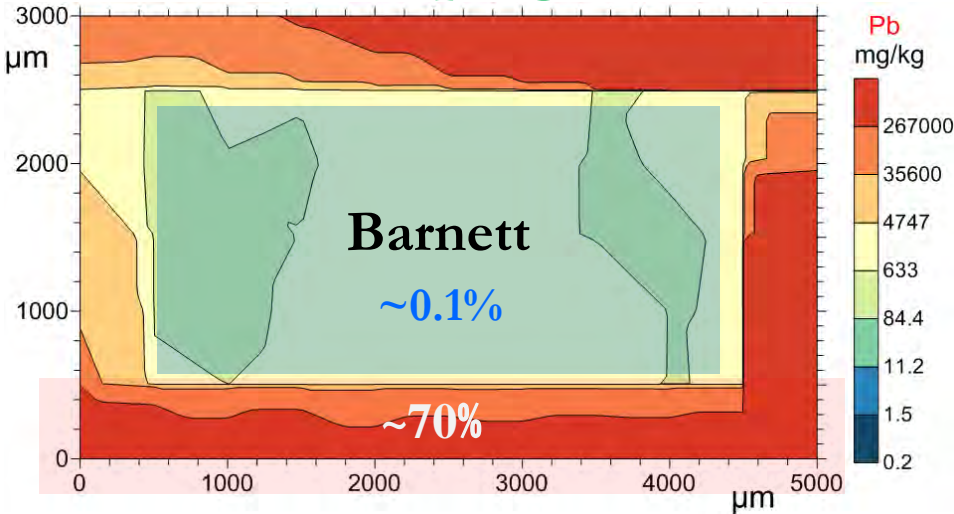
- IPA [zwittering]

- ✓ MoO₄²⁻ (0.553 nm)
- ✓ Ru-complex (2.42 nm)

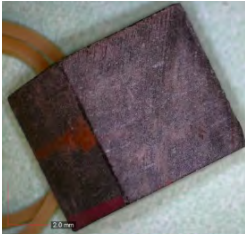


Low Pore Connectivity of Mudrock: Multiple Evidence

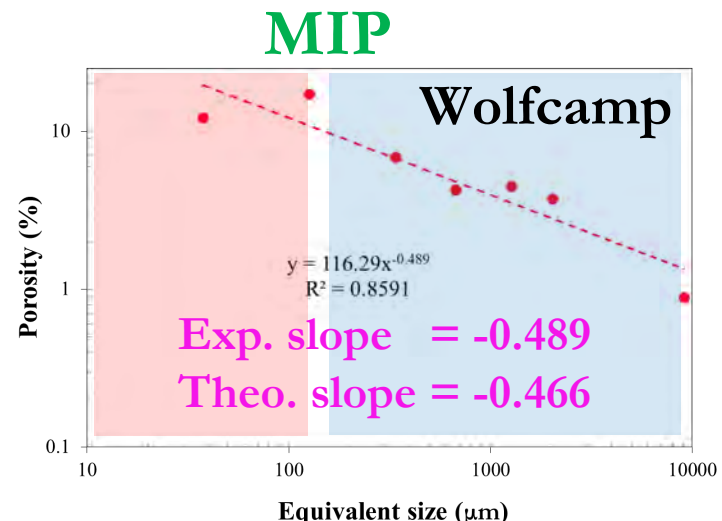
Wood's metal impregnation (400 MPa)



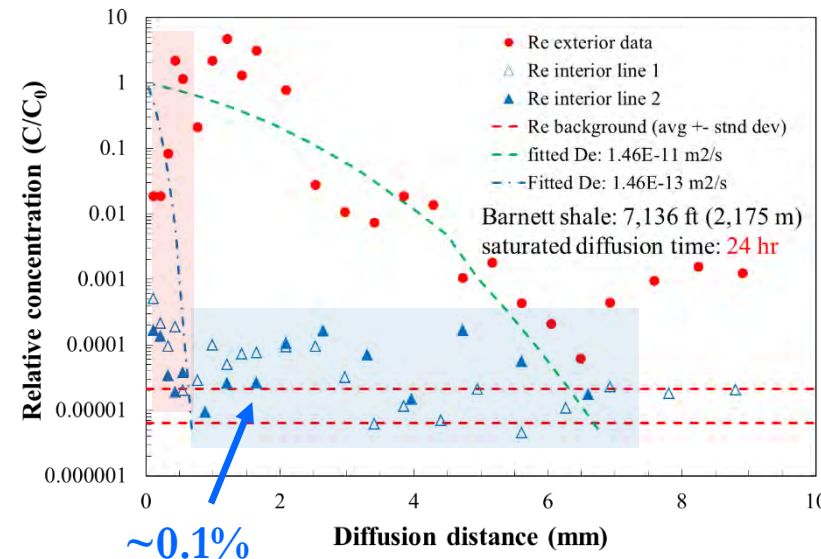
1 cm cube



Size GRI (500-841 μm)



Diffusion Barnett

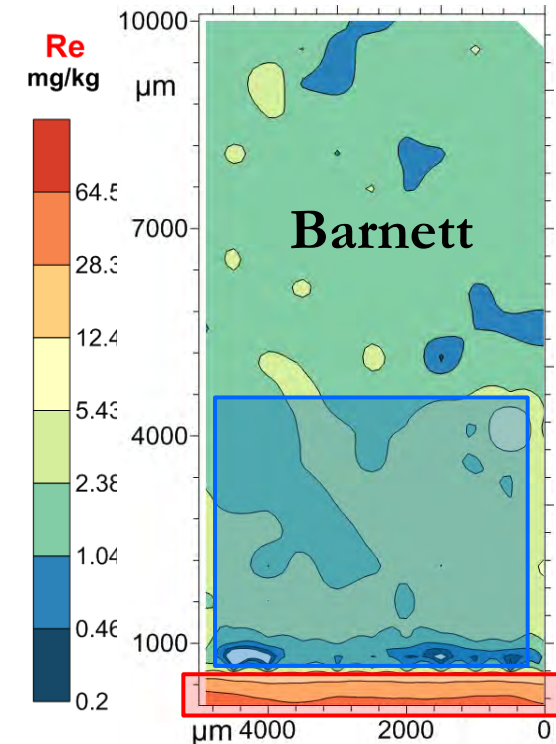


Unique “Dual-Connectivity Zones”

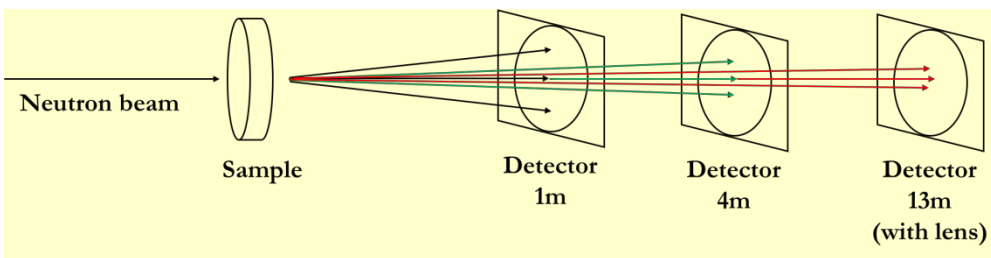
“Surface Zone”

“Bulk Zone”

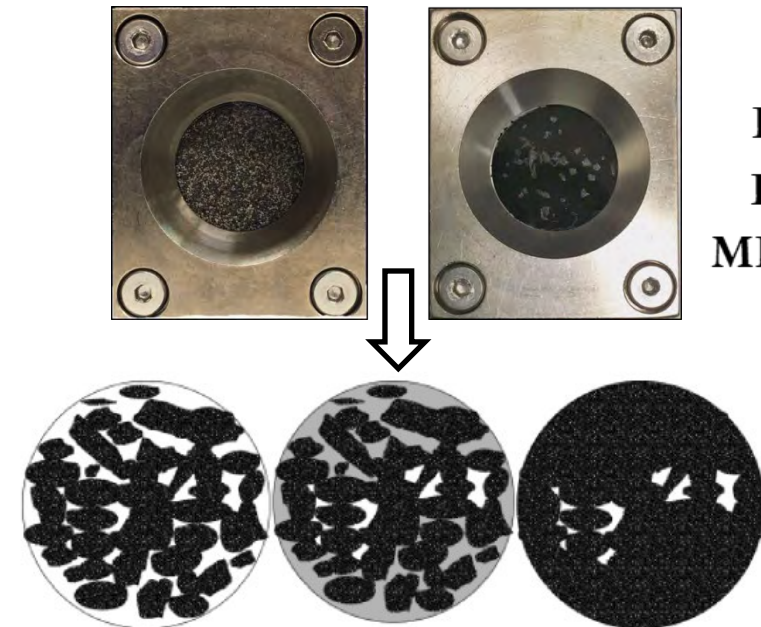
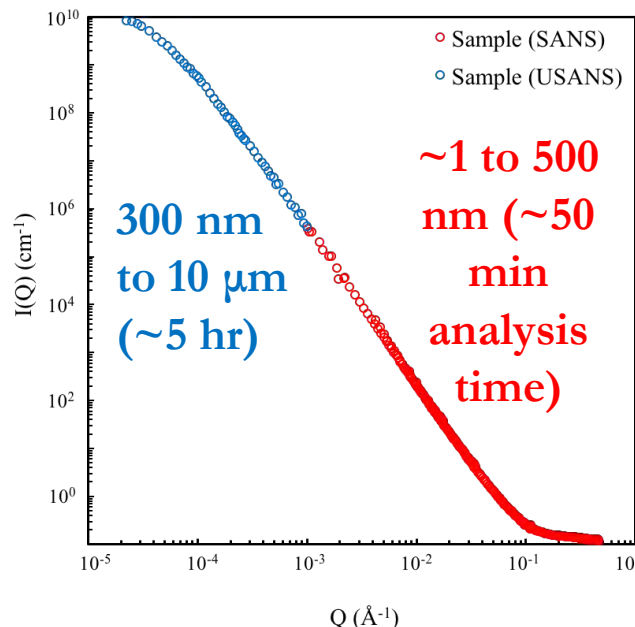
Imbibition



Small Angle Neutron Scattering (SANS): Contrast Matching



- Detect both connected and closed pores
- Obtain full-scale nm- μ m pore diameters
- Quantify hydrophilic vs. hydrophobic pore space
- Investigate reservoir P-T condition



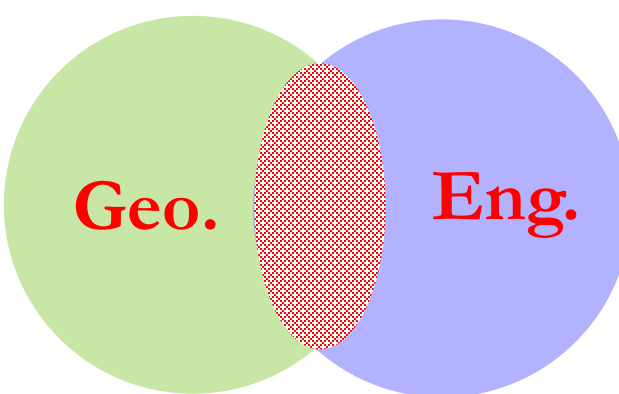
Porosity Results(%)

mudrock	Sample 1	Sample 2	Sample 3
Total	11.4	7.83	9.28
Hydrophyllic	7.04	2.7	7.16
Hydrophobic	4.92	2.58	2.32
MICP Accessible	2.12	0.79	3.71

d-H₂O
d-2DT
d-IPA

- Yang et al., Fuel, 2017
- Sun et al., IJCG, 2017
- Zhao et al., SR, 2017
- Zhang et al., MPG, 2019
- Zhang et al., IJCG, 2019
- Zhang et al., GRL, 2020

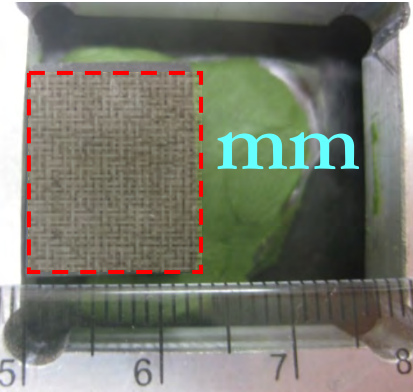
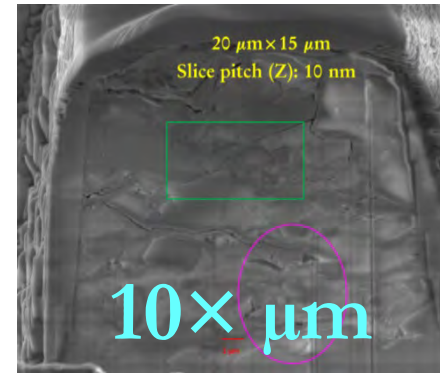
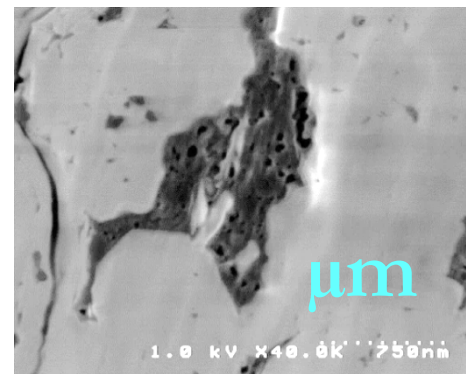
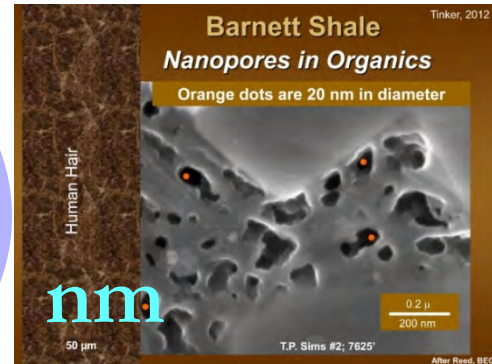
Improved Understanding of Hydrocarbon Recovery Across Scales



Geological
Sweet
Spots



Engineering
Sweet Spots



wettability

accessibility

tortuosity

capillarity

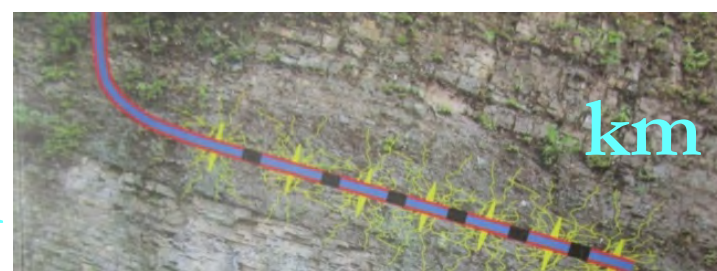
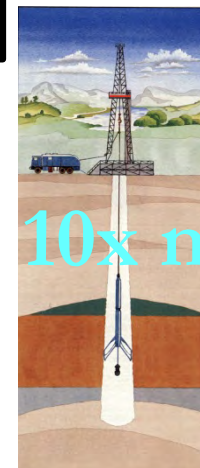
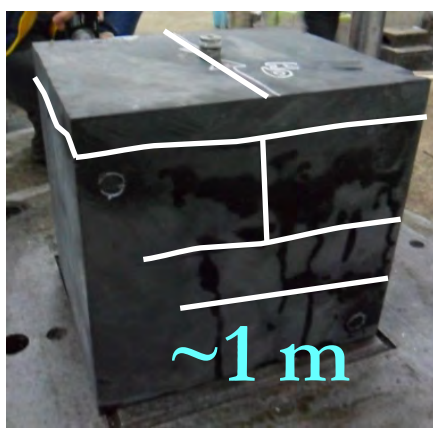
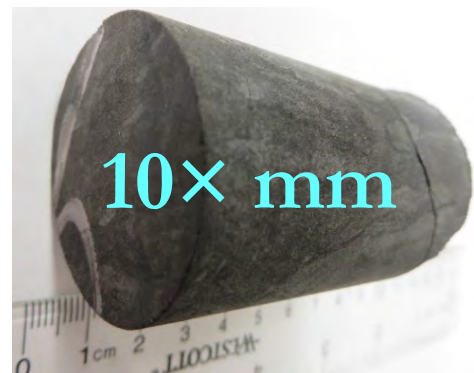
Fracture-Matrix interaction
→ productivity

fracability

diffusivity

permeability

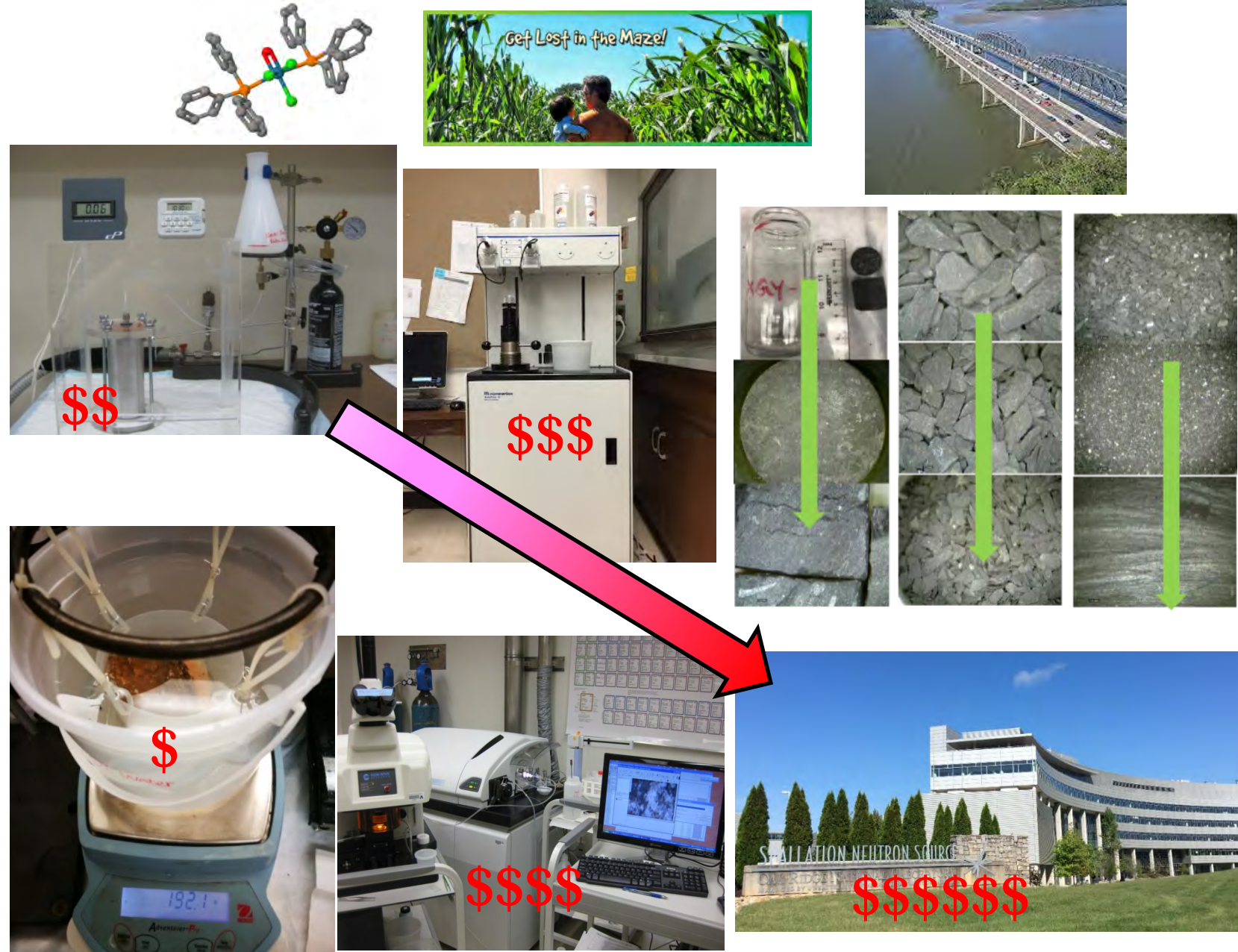
deliverability



Pilot hole with logging
and core samples

Summary

- Nano-petrophysical studies (properties of rock and fluids, as well as their interactions)
- Matrix pore-throat sizes: tight oil movability (5-50 nm; siltstone)
- “Dual connectivity” zones at ~400 μm from sample edge
- Mixed wettability at μm scale, more oil-wet than water
- Dual flow paths in 3-D space: >10-50 nm hydrophilic pore network at slow rate; ~5 nm hydrophobic pore network with rapid rate but size exclusion
- Co-mingling layers of source rocks, reservoirs, and carrier beds in Permian shale systems



Acknowledgments

